# GAIT MECHANICS, JOINT CONTACT FORCES, AND MUSCLE FORCES IN OLDER ADULTS WITH RADIOGRAPHIC KNEE OSTEOARTHRITIS AND KNEE PAIN COMPARED TO A SIMILAR POPULATION WITH NO RADIOGRAPHIC KNEE OSTEOARTHRITIS

BY

JOSHUA F. WALLACE

A Thesis Submitted to the Graduate Faculty of

WAKE FOREST UNIVERSITY GRADUATE SCHOOL OF ARTS AND SCIENCES

in Partial Fulfillment of the Requirements

for the Degree of

MASTER OF SCIENCE

Health and Exercise Science

December, 2014

Winston-Salem, North Carolina

Approved By:

Stephen P. Messier, Ph.D., Advisor

Daniel P. Beavers, Ph.D., Chair

Paul DeVita, Ph.D.

ACKNOWLEDGEMENTS

I would like to thank my advisor, Dr. Messier, for his continuous support throughout my master's study and research. His guidance and criticism have pushed me to be a better writer, researcher, and student.

I would also like to thank the rest of my thesis committee: Dr. Daniel Beavers, and Dr. Paul DeVita for their insightful comments, helpful advice, and patience with rescheduling thesis defense dates.

My sincere thanks to Jovita Newman and Ryan Hill who helped me find and contact participants, coordinate the study, and answer my endless stream of questions. Their help has been invaluable to me throughout the process. Thank you to all the lab staff for everything from MATLAB to finding participant files.

A special thank you to Jason Pifer and the WFU Chemistry Department for keeping me sane over these past two years.

# Table of Contents

LIST OF ILLUSTRATIONS AND TABLES

## LIST OF ABBREVIATIONS

| | |
|---|---|
| AP | Anterior-posterior |
| APGRF | Anterioroposterior Ground Reaction Forces |
| BMI | Body Mass Index |
| CoM | Center of Mass |
| CVD | Cardiovascular Disease |
| DEXA | Dual-energy X-ray Absorptiometry |
| EMG | Electromyography |
| GRF | Ground Reaction Forces |
| GS | Gastrocnemius-soleus |
| JRF | Joint Reaction Force |
| K-L Scale | Kellgren-Lawrence Grading Scale |
| OA | Osteoarthritis |
| PCA | Physiologic Cross-section Area |
| Q-Angle | Quadriceps Angle |
| ROM | Range of Motion |
| RRA | Residual Reduction Algorithm |
| SIMM | Software for Interactive Muskuloskeletal Modeling |
| START | Strength Training and ARthritis Trial |
| VAS | Vastus |
| VGRF | Vertical Ground Reaction Forces |
| WOMAC | Western Ontario and McMaster Universities Arthritis Index |

# ABSTRACT

*Phase I*

*Objective:* Compare joint contact forces, ground reaction forces (GRF), and muscle forces during walking between older adults with knee radiographic osteoarthritis and pain due to OA (OA group) to adults with knee pain but no radiographic OA (non-OA group).

*Methods:* Data were collected from 6 non-OA participants and compared to 15 OA participants who both underwent a 3-dimensional gait analysis. Outcomes include peak range of motion of the hip, knee, and ankle in the sagittal plane, peak internal hip and knee abduction moments, and total moment and power in the sagittal plane. A mixed linear model approach controlling for age, and gender was used to compare characteristics across OA groups, and to estimate biomechanical gait characteristics.

*Results:* There was a significant difference in the peak total moment in the sagittal plane ($P = 0.02$) between the two groups. All other variables showed no significant difference.

*Conclusion:* Our results suggest there is no significant difference in altered gait mechanics between the two groups. A larger number of participants are needed to make results more powerful.

*Phase II*

*Objective:* Compare a musculoskeletal model, OpenSim, that calculates 76 muscle forces in the lower extremity [85] to a lumped muscle model that has been validated and used in previous studies [73].

*Methods:* Previously collected data from 31 participants in the START study were run through both musculoskeletal models. Outcome variables included peak internal AP shear and compressive forces of the knee, quadriceps, hamstring, and gastrocnemius peak muscle forces. Values were compared using mixed model approach controlling for within person variability.

*Results:* There was a significant difference between 2$^{nd}$ peak AP shear forces ($P < .01$), 2$^{nd}$ peak compressive force ($P < .01$), peak quadriceps muscle force ($P < .01$), peak hamstring muscle force ($P < .01$), and peak gastrocnemius muscle force ($P < .01$).

*Conclusion:* Our results demonstrate that the two musculoskeletal models will not produce the same resultant muscles forces. Results from other studies support our findings from both models, however, the DeVita model has been used in previous studies with knee OA participants and has shown similar results to those by Fregly et a

# Literature Review

## Introduction

Osteoarthritis (OA) is the most common joint disorder affecting adults ages ≥ 65 years [51]. The prevalence of knee OA is an estimated 250 million adults worldwide or 3.6% of the world population [92]. In 2005, an estimated 27 million adults had OA in the United States [27]. Prevailing symptoms include joint locking, effusion, stiffness, and tenderness [26]. This will often lead to chronic pain, expensive treatments, and disability that can result in job loss and social isolation. OA can affect any joints of the body; however, OA of the knees has a significantly larger social and financial impact on the inflicted [53]. In 2004, the Center for Disease Control and Prevention estimated $14.3 billion in costs related to total knee replacements due to OA [53].

Henriksen et al. found that a group of participants with knee OA had similar gait characteristics to those with healthy knees after being injected with lidocaine [110]. This suggests that pain cause altered gait in those with knee OA. However, there are no studies that have determined whether the structural damage caused by knee OA has any effect on gait, independent of pain.

High speed video systems are used to analyze gait. We have used gait analysis to assess human movement in knee OA and healthy adult populations [93], [80], [81]. The kinematic data derived from the video analysis, in conjunction with kinetic data from a force plate, can be used in musculoskeletal models to yield joint contact forces during movement. More advanced models are able to divide the larger joint contact vector into smaller muscle vectors using inverse dynamics along with either an optimization routine, or gathered electromyographical data [8]. This gives a better representation of the joint in

question, can be useful in examining how different conditions alter gait, and can add important clinical information when prescribing a treatment a plan [64].

This study had two goals: (1) to compare joint contact forces, ground reaction forces (GRF), and muscle forces during walking between older adults with knee radiographic OA and pain due to OA to adults with knee pain but no radiographic OA; and (2) to compare a musculoskeletal model, OpenSim, that calculates 76 muscle forces in the lower extremity [85] to a lumped muscle model that has been validated and used in previous studies [73].

The first aim of the study is to compare the sagittal plane joint range of motion of the hip, knee, and ankle, peak adduction moments of the hip and knee, total moment in the sagittal plane, total power in the sagittal plane, walking speed, stride length, and stride rate of older adults with knee OA and pain to that of a similar population with reported knee pain and no knee OA. We will also compare the asymmetry of vertical GRF (VGRF), anterioroposterior GRF (APGRF), step length, and maximum loading rate between the most affected and the least affected leg of each participant in the OA group. It is hypothesized there will be no significant difference in gait between patients with radiographic knee OA and knee pain compared to those with knee pain but without radiographic knee OA.

The second aim of the study is to compare knee shear and compressive forces, as well as muscle forces of the hamstrings, quadriceps, and gastrocnemius from the OpenSim model [83] to that of the DeVita model [73]. It is hypothesized that there will be no significant difference between the two models.

## Musculoskeletal Modeling

### Inverse Dynamics

Inverse dynamics is an approach used to determine joint kinetics given kinematic and external kinetic data. Inverse dynamics uses known kinematic and inertial properties of the body to determine joint forces and moments. While it is possible to perform a full body calculation, the process is greatly simplified if one body segment is considered at a time [9]. A distal body segment, such as a foot or hand, is chosen as a starting point for calculations. The known movement and inertial data of the individual body segment are used to solve for the joint reaction forces and internal joint moments at the proximal end of the limb. The next proximal limb is considered in the same manner with the addition of the previously calculated forces and moments from the more distal limb. If the subject is performing an action, i.e. throwing a ball, walking, running, etc., the external force generated must also be considered in the first calculation [7].

The only equations needed for this method are $F = ma$, and $M = I\alpha$ where $F$ is the force exerted on the joint, and $M$ is the internal moment acting on the joint. The remainder of the variables are all dependent on the body segment being examined where $m$ is the mass, $a$ is the acceleration, $I$ is mass moment of inertia, and $\alpha$ is the segment angular acceleration. The advantages to this method are it is relatively easy to execute and validate [82]. Despite its ease of use, inverse dynamics has its limitations: it does not account for co-contraction and it does not estimate muscle forces.

## Marker System

Currently, the gold-standard for gait analysis is placing passive or active markers over predefined anatomical landmarks, and filming their movement using an array of high-speed cameras [55]. A passive marker system involves using markers with a reflective surface in tandem with cameras that emit an infra-red light. The infra-red light is emitted through diodes that surround the lens of the camera that reflect off the markers to the lens and distinguished using recognition software [5]. An active marker system uses markers that give off an infra-red signal that is then picked up by the cameras. There are known advantages and disadvantages to both systems. The active marker system allows for sampling at higher frequencies, and provides less error and artifact from infra-red light reflecting off of the environment. However, the passive system does not require the participant to be attached to wires or carry a battery pack [6]. This advantage alone is enough to make the passive system preferential in a research setting as it does not run the risk of altering gait.

## Modeling

Scientific models are an important tool used to explain and more clearly define an aspect of our universe. All models have similar end goals, which are to visualize, predict, quantify, and understand an event. Models can be categorized into two broad areas based on what they represent: models of phenomena, and models of data. Models of phenomena describe or represent a topic in a form we can more easily understand. A few examples of this are a scale model of a building, the Bohr atom model, and the Global Economic model. Models of data are created from raw data that have been collected. Outliers in the

raw data are then removed and a smooth curve is fit to the points. This is done to make the data more ideal to examine. A common example is predicting the trajectory of a planet. Models are not limited to just one category, and may have aspects of both phenomena and data models [1]. Musculoskeletal modeling is a data model. It collects raw kinematic and kinetic data which is filtered. Curves are fitted and smoothed during post-processing to give a more accurate representation of human movement.

The fundamental purpose of a musculoskeletal model is to determine joint contact forces, joint moments, and muscle forces in vivo. This is accomplished using a combination of kinematic and kinetic data collected via gait analysis. Post-processing is done to remove artifacts that may have been picked up during collection from excess movement of clothing or skin on which the markers were placed. Inverse dynamics is used to determine joint moments and joint contact forces [2]. Finally, the model is validated using torque data, electromyography (EMG) data, and/or comparing results with previously used models [3].

A model of interest in this study was created in a joint effort by Darryl Thelen, Ajay Seth, Frank Anderson, and Scott Delp; it is adopted from the model created by Delp et al. [65]. This model consists of 92 musculotendon actuators that represent 76 muscles of the lower extremity and torso. OpenSim is open source software that allows interaction and modification of musculoskeletal models. Open source software permits users to edit the source code of the software, and distribute it freely without any technical or copyright limitations. Consistent community updates and contributions allow programs such as OpenSim to become more robust and available to anyone who wishes to use it [66].

Anthropometrics

Dimensions and behavior of bones, joints, and muscles in the model are constructed based on anthropometric data gathered from other studies. For the model used in this study, bone geometry for the ankle and shank were adopted from Stredney et al. [88]. Geometry for the pelvis is created using a polygon mesh and assessing the coordinate positions using a three-dimensional digitizer.

Muscle and tendon paths are defined by an array of line segments that run from origin to insertion point for each muscle. Some muscles, such as the quadriceps tendon, wrap around other structures. A wrapping point is created to allow the line segment to bend about a point rather than pass through structure. Peak isometric force is determined using the physiological cross-sectional area of a muscle taken from Friederich et al. who used a 37 year old male and a 63 year old female cadavers, [90] and Wickiewicz et al. [89] and follow the same methods used by Hoy et al. [91]. These peak forces are important in ensuring a muscle actuator remains true to the muscle it represents and does not generate a force that is physiologically impossible. Optimal fiber length and pennation angle are largely taken from Wickiewicz et al. and scaled by a factor of 2.8/2.2 determined by the ratio of sarcomere length where peak force is developed by muscle fibers based on the sliding filament theory of muscle contraction (2.8 micrometers) to the sarcomere length (2.2 micrometers) [89]. Muscle data from Friederich et al. [90] were used for muscles not reported by Wickiewicz.

To have a more accurate representation of a subject, the model must be scaled based on subject-specific anthropometrics. Some common limb segment parameters

include: length, mass, density, center of mass location, mass moment of inertia, and radius of gyration of the limb segment. The difficulty in obtaining these values varies. The procedure for measuring limb length involves measuring from one predefined anatomical landmark to another. Obtaining other measurements such as segment center of mass location or density can be more difficult. Computational methods take input variables such as limb length and radius and output limb segment volume [32]. More refined techniques may be used to obtain a more accurate value, for example, using Dual-energy X-ray absorptiometry (DEXA) and Software for Interactive Muskuloskeletal Modeling (SIMM) can more accurately report bone mineral density and tendon slack length respectively [34], [33].

Model Validation

As the application of musculoskeletal models in a clinical setting increase, the importance of validating the model becomes more apparent. Model validation is important to ensure the values obtained from the model are accurate given the physiological constraints [3]. A commonly used technique for validating a model is to compare the model's predictions to a previously published study or model that examines the same information [10]. Another method is to validate using EMG signals. This method is particularly useful for models that predict muscle forces due to the direct measurement of muscle excitation gained from the EMG [8]. The coefficient of determination, or $R^2$, is used to determine the correlation between outputs of the new and old models. A $R^2$ value will fall in the range of 0 and 1 where 0 indicates no correlation between models while 1 expresses a perfect match between the two models' output [84].

Another method of model validation is to compare model results to reported values of instrumented total knee replacement made available by Fregly et al. These participants had a mean age of 83 years, mass of 64.6kg, and 166cm tall [112]. This data has been compared to results from the model created by DeVita have shown to be highly similar [73], [113].

**Knee Anatomy**

The knee is a versatile joint due to its ability to provide stability while extended, and mobility while flexed [11]. It is composed of three articulations: the tibiofibular joint, the tibiofemoral joint, and the patellafemoral joint [12]. The tibiofibular joint is composed of the articulation between the head of the fibular and the posterolateral and inferior aspect of the tibial condyle. It moves with a gliding motion which is based on the rotation of the foot and tibia. The main function of this articulation is to dissipate torsion generated by the foot [13].

The tibiofemoral joint is the articulation between the femur and the tibia and is often considered the knee joint. Flexion and extension are the primary movements; however, there is a small but significant amount of rotation. This joint is classified as a modified hinge joint due to its combination of hinge and pivot type joints [11]. One of the main contributors to the knee joint's mechanical nature is how the lateral and medial condyles of the femur are shaped. The lateral condyle is aligned with the femur, is flatter, projects more posteriorly, has a larger surface area, and is more prominent anteriorly to help hold the patella in place. The medial condyle is angled away from the femur on the posterior side, is aligned with the tibia, projects more distally and medially, and is longer

in the anteroposterior direction. This structure allows the knee to be mobile during flexion/extension, internally rotate as full extension is reached, and is stable once fully extended [12].

The meniscus is a cartilaginous tissue found in the joint space of the knee and is divided into two segments; the lateral and medial meniscus. The lateral meniscus has an oval shape, consumes more space, and is more mobile than the medial meniscus. The anterior meniscofemoral ligament and posterior meniscofemoral ligament both originate from the posterior horn of the lateral meniscus, and travel behind the posterior cruciate ligament to the medial femoral condyle. The medial meniscus has a crescent shape and is attached anteriorly to the anterior cruciate ligament, and the tibial collateral ligament laterally [14].

The main purpose of both menisci is to act as a shock absorber for forces that travel through the knee, particularly tension and torsion forces [15]. They are wedge-shaped with the thicker part towards the surface of the joint and become narrower as they travel to the joint center. This shape gives an increased contact surface for the tibia which can absorb up to half of the weight-bearing load during full extension and some during flexion [17]. When the meniscus is removed, the contact area in the joint is reduced by approximately two thirds. This will increase the risk of injury due to the increased load per unit of area across the contact sites [18]. The periphery of the meniscus is vascularized which allows it to heal if damaged. The inner portion, however, lacks vascularization making deeper tears much more serious as they do not heal [16].

The patellofemoral joint is composed of the articulation of the trochlear groove of the femur with the patella. The patella is a sesamoid bone surrounded by the tendons of the quadriceps femoris. The main purpose of this bone is to increase the leverage that the previously mentioned tendons can exert on the femur. This is done by increasing the angle at which these tendons act [19]. The patellar tendon connects the patella to the tibial tuberosity. Patellofemoral and patellotibial ligaments connect the patella to their respective bones.

The quadriceps angle (Q-angle) helps determine the position of the patella as well as the alignment of the lower limbs in the frontal plane. The Q-angle can be found by drawing a line from the anterior superior spine of the ilium to the middle of the patella, and another from the middle of the patella to the tibial tuberosity [21]. Normally, the hip should align vertically over the knee joint. Males typically have a Q-angle between 10° to 14° while females are between 15° to 17° [20]. A Q-angle below the range is considered genu varum while Q-angles above the range are classified as genu valgum. Genu varum, or varus knee alignment, puts more strain on the medial compartment of the knee joint. Genum valgum, or valgus knee alignment, causes more force to be exerted on the lateral aspect of the knee. Both varus and valgus knee alignment have been shown to increase knee osteoarthritis progression in the medial and lateral compartment of the knee respectively [22], [23].

During normal walking, the loading response on the knee consists of knee flexion controlled by an extension moment from heel strike to midsupport. A flexor moment is generated in the second half of the stance phase, which is followed up by a small

extension moment. There is very little torque and power generated at toe off until the end of swing phase, where flexor moments act to control extension of the shank [79].

Knee Motion

The knee can flex up to 130° to 145° and hyperextend to 1° to 2°. There is 6° to 30° of internal rotation about the medial intercondylar tubercle of the tibial plateau throughout 90° of flexion [24]. Abduction and adduction range of motion is relatively small, being no more than 5°.

Chronic pain will lead to alterations in gait due to a decrease in muscular strength and pain avoidance [75]. One significant difference is an increased external adduction moment at the knee joint [76]. This greater moment leads to an increase in compression forces on the medial aspect of the knee and can hasten the breakdown of cartilage in the joint [77]. Another observed change in gait is a decrease in average walking speed which has been linked to survival in older adults [78].

**Figure 1:** Angular displacement, and moments of the knee joint during a single walking stride [79].

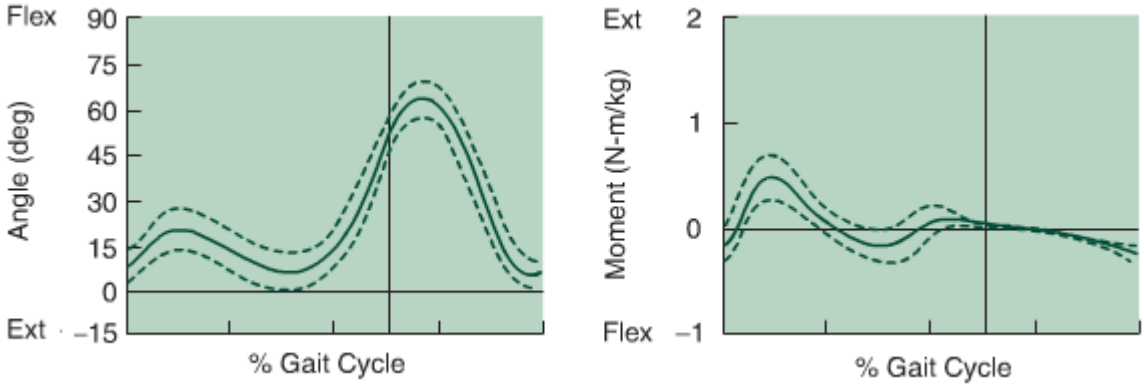

## Pathogenesis of Knee Osteoarthritis

Osteoarthritis is often referred to as a set of abnormalities that cause degeneration of joints. Normally, bones at the knee joint articulate with one another, aided by the presence of the meniscus. This white fibrocartilage distributes joint forces over a larger surface area, and helps to stabilize the joint in flexion and extension [86]. After the onset of OA, the surface layer of the meniscus degenerates. This lowers the contact area in the joint which causes an increase in the amount of pressure the tibia and femur exert on each other [87]. Eventually, bits of bone will break away and float in the joint space. Bone spurs, also known as osteophytes, will grow on the edge of the joint. All of these factors cause swelling, loss of motion, and pain within the joint [28].

OA is often referred to as the non-inflammatory disease to separate it from other inflammatory arthritis' such as rheumatoid arthritis. Despite this nomenclature, inflammation is widely recognized as a contributing factor to OA progression [29]. One inflammatory related factor is synovitis, which is the inflammation of the synovial membrane. Synovitis occurs when the synovial membrane is invaded by mononuclear cells and proinflammatory mediators such as interleukin 1[beta], tumor necrosis factor-[alpha], and chemokines are produced [30]. These cytokines have an effect on the degradation of cartilage [31].

### Risk Factors

While the exact cause of OA is unknown, there are a set of established risk factors. Obesity, knee alignment, age, gender [35] [42] [41], ethnicity [35], joint trauma, and occupation are some of the leading risk factors. Obesity is a significant contributing

factor to OA due to altered gait and physiological conditions [44-47]. The Framingham study showed men who were in the heaviest quintile of weight had an increased risk of knee OA with a relative risk of 1.51, while women in the heaviest quintile had a relative risk of 2.07 [45]. Felson et al. found that the effects of body mass index (BMI) on knee OA progression increased with moderate varus or valgus malalignment of the knee [44]. Varus knee alignment has a more severe impact on the development of knee OA compared to valgus alignment. This is due to the distribution of force from the ground being focused on the medial tibial and femoral condyles [46]. The same phenomenon only occurs in the lateral compartment of the knee with severe valgus knee alignment [47]. An increase in thigh circumference, which often accompanies obesity, will cause a person to have a wider stance. Donelan et al. found that an increase in stance width yields a greater knee adduction torque which can increase joint contact force in the medial compartment of the knee [48] [49].

Aging is a strong contributing factor to the incidence of OA [35] [43]. Gender has also been shown to be an important risk factor. Women have a higher prevalence rate of 42.1% compared to men who have 31.2% [42]. Men also have a 45% lower risk of incident knee OA [109]. Even women who have a genetic aversion to knee OA are at greater risk compared to their male counterparts [41]. Some common occupational risk factors for knee OA are overexposure to biomechanical stressors which include excessive squatting or kneeling, jumping, standing for more than two consecutive hours per day, vibration, lifting more than 10kg, routine stair climbing, and walking further than 3km per day [36], [37], [38]. While it is not entirely understood, a genetic factor has been found with OA [39], [40]. Spector found heritability of knee OA to be 40% [39]. Multiple

studies, conducted by Valdes, have shown the presence of numerous genetic variants can significantly increase the risk of knee OA [40], [41].

## Methods

This study consisted of two phases. The goal of Phase I was to compare the differences in gait between a group of older adults with chronic knee pain and radiographic knee OA (OA), and a matched cohort with knee pain but no radiographic knee OA (non-OA). It was hypothesized there was no significant difference in gait between the groups. Phase II compared the gait kinetics derived from two musculoskeletal models, OpenSim [85] and DeVita [73]. The phase II hypothesis stated there was no significant difference between the compressive, and shear joint-contact forces, quadriceps, hamstrings, and gastrocnemius muscle forces of the two models.

### Participants

Subjects that participated in Phase I of the study were selected from a cohort of the Strength Training and ARthritis Trial (START). The non-OA group was evaluated for the START study, but did not qualify for participation because they did not have radiographic knee OA determined by the Kellgren-Lawrence Grading Scale (K-L scale), although they had a qualifying Western Ontario and McMaster Universities Arthritis Index (WOMAC) pain rating of 4 or greater on a scale from 0-20, and had a BMI of 30 $kg/m^2$ or less. Six people agreed to participate. The OA group consisted of fifteen participants who were enrolled in the START study, had a K-L score of 2 or 3, a WOMAC pain score of 4 or greater, and had a BMI of 30 $kg/m^2$ or less.

All data used in Phase II of the study was previously collected during the START study. Thirty-one participants who had a BMI of 30 or less were randomly selected.

**Phase I**

All data were collected and processed in the J. B. Snow Biomechanics Laboratory. Kinematic data were collected using a 6-camera Motion Analysis Corporation System set at a sampling rate of 100Hz. A 53 passive marker system was used using a modified Cleveland Clinic setup. The data were collected, tracked, and edited with Cortex 3.0 software, then filtered with a Butterworth low-pass filter with a cut-off frequency of 6Hz. Kinetic data were simultaneously collected with 2, 6-channel AMTI force platforms with sampling rates of 1000Hz.

Participants were given an informed consent, briefed on the testing protocol, and what was expected of them before any testing occurred. The participants wore New Balance Barringer 890 neutral lightweight trainers to control for the effects of footwear. A photocell control system interfaced with digital timers developed by Lafayette Insturment Co. was used to measure walking speed. Participants were asked to walk across the runway at their normal walking pace six times to obtain their average walking speed. This speed was used in all subsequent trials.

Reflective markers were placed on the participants according to the setup outlined in Appendix B. Markers were first placed in accordance to the full body static setup. The participant was then asked to stand on the second force plate in anatomical neutral position with their upper arms abducted 45°. A static calibrated trial was recorded, and all static markers removed to match the full body walk setup. Another static trial, known as the static no calibration trial, was taken. All markers were then labeled in Cortex to identify the appropriate markers during testing.

Three successful trials were collected on each participant for subsequent analysis. A successful trial was defined as placing each foot in its entirety on a force platform during a normal walking stride while maintaining walking speed within the estimated range (±3.5). A complete heel strike to toe-off on the force platform was considered a successful strike of the foot.

The height of the participant was measured with a statiometer. The participant was instructed to stand erect with heels and back against the wall while looking straight ahead. Height was measured to the nearest 0.1cm. The participant's weight was measured using a manual scale manufactured by Health O Meter, Inc. Weight was taken to the nearest 0.1kg. The participant was dressed in light clothing and was not wearing shoes during both measurements.

**Phase II**

Kinematic and kinetic data of 30 participants were processed using two musculoskeletal models. The first was created by DeVita and Hortobagyi [73] and calculated knee joint (tibiofemoral) compressive and anterior-posterior (AP) shear forces, patellofemoral force (the compressive force between the femur and the patella), and quadriceps, hamstrings and gastrocnemius muscle forces. The second model used was developed by Thelen et al. [85] and came packaged with OpenSim. Up to 76 muscles are represented in the lower extremity. For the purposes of this study we observed 9 muscles: rectus femoris; vastus medialis; vastus intermedius; vastus lateralis; semimembranosus; semitendinosus; the longhead of the biceps femoris; and the lateral and medial gastrocnemius. A full description of each model is presented below.

DeVita Model Description

The model created by DeVita and Hortobagyi has three main procedures. The first is to use inverse dynamics to calculate joint torques and joint reaction force (JRF) of the hip, knee, and ankle using inverse dynamics. The DeVita model assessed the mass, center of mass, and inertial properties of limb segments based on a mathematical model presented by Hanaven et al. [67] and relative segmental masses reported by Dempster et al. [68].

The second step was to determine muscle forces in the gastrocnemius, hamstrings, and quadriceps. In calculating the gastrocnemius force, it was assumed that all plantar/flexor torque originated from the gastrocnemius-soleus (GS) and there was no co-contraction of anterior muscles. Moment arm values for the muscle were determined from previous literature [71]. The plantar flexor torque was divided by the moment arm of the Achilles tendon to calculate the GS force. The GS force was multiplied by the cross sectional area of the gastrocnemius to obtain the force generated by the gastrocnemius. The direction the gastrocnemius force was traveling was determined by the knee and heel marker positions and was represented as $\alpha$.

Two assumptions were made when calculating hamstring muscle force. The first was that the force vector is parallel with the femur and at an angle $\beta$ to the tibia. This is based off of coordinate mapping conducted by White et al. [72]. The second assumption is that no co-contraction of the hip flexors occurs during the initial part of stance. The extensor torque at the hip was used to calculate the hamstring muscle force. It can be represented as:

$$Hp = \left(Ham \frac{PCA}{Ham\ PCA + GM\ PCA}\right) * (Hd * GMd)$$

where *Hp* is the proportion of the hip extensor torque generated by the hamstrings, *Ham PCA* and *GM PCA* are the hamstrings and gluteus maximus physiologic cross-section area (PCA), and *Hd* and *GMd* are the hamstrings and gluteus maximus moment arms respectively. These values were also obtained from previous literature [73]. The hamstring force was then found by dividing *Hp* by *Hd*.

The quadriceps muscle force was calculated using knee joint torque, hamstrings, and gastrocnemius muscle forces. The quadriceps and gastrocnemius muscle forces included in this calculation take co-contraction into consideration. Knee joint torque was the net torque at the knee shown by:

$$Kt = Q(Qd) - H(Hd) - G(Gd)$$

where *Kt* is the net knee torque, *Q*, *H*, and *G* are functions of the quadriceps, hamstrings, and gastrocnemius muscle forces as a function of their respective moment arms. The equation can then be rearranged to solve for *Q*:

$$Q = \frac{Kt + H(Hd) + G(Gd)}{Qd}$$

The quadriceps force vector, □, was also established using previous literature [74].

The final step in this model was calculating the knee joint forces. All forces acting vertically were summed for the knee joint compressive force, while all forces acting horizontally were summed to find the knee joint shear force in the anteroposterior direction yielding the following equations:

$$Ks = Gsin(\alpha) - Hsin(\beta) + Qsin(\phi) - Kzsin(\lambda) + Kycos(\lambda)$$

and

$$Kc = Gcos(\alpha) - Hcos(\beta) + Qcos(\phi) - Kzcos(\lambda) + Kysin(\lambda)$$

Where *Ks* is the shear force, *Kc* is the compressive force, *Kz* is the JRF in the vertical direction, and *Ky* is the JRF in the horizontal direction.

**Figure 2:** Visual representation of the DeVita Model with muscle forces and angles.

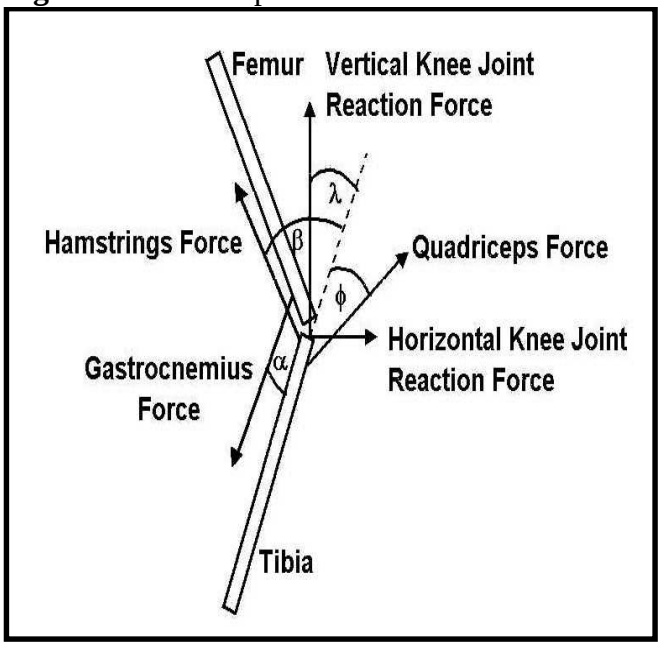


OpenSim Model

Yamaguchi et al. (1989) developed a single-degree-of-freedom model to calculate the extensor moment arm of the knee in a more computationally efficient way [74]. This model was adopted by Delp et al. and used to specify transformations between the femoral, tibial, and paterllar reference frames as functions of the knee angle. The femoral condyles are represented as ellipses while the tibial plateau is illustrated as a line segment. Transformation from the femoral to the tibial reference frame was established in such a

way that the femoral condyles remain in contact with the tibial plateau throughout the knee range of motion (ROM) [65]. The tibiofemoral contact point is dependent on the knee angle and is specified according to data reported by Nisell et al. (1986) [105]. The model used by Delp et al. is shown in Figure 3 where $F_q$ is quadriceps muscle force, $\theta_k$ is the knee angle, □ is the patellar ligament angle, $\beta$ is the angle between the patella and the tibia, and $\ell_{pl}$ is the length of the patella ligament which is considered constant [65].

**Figure 3:** Geometry to determine knee kinetics and kinematics in the sagittal plane used by Delp et al. (1990).

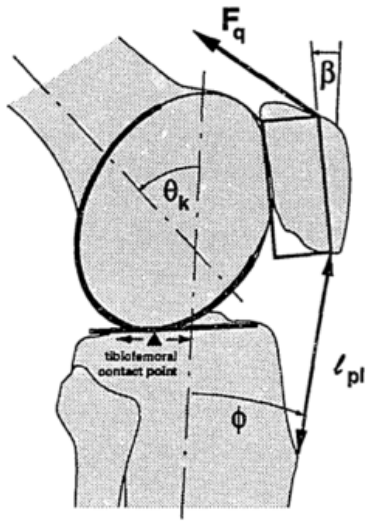


92 musculotendon actuators make up a total of 76 muscles in the lower extremity. These actuators are represented by line segements defined by anatomical landmarks on the bone surface models. In the case when a muscle does not travel in a straight line, a "wrapping point" is introduced to allow the muscle to curve around any obstacle it may encounter. This happens once the knee is flexed more than 80° and the quadriceps wraps around the distal aspect of the femur. As the knee flexes more, more "wrapping points" are introduced to prevent the muscle force from passing through the bone. This concept is applied any muscle that bends throughout motion.

Inertial properties are adapted from a model developed by Anderson and Pandy (1999) and are scaled by a factor of 1.05626 [100]. The anthropometrics of their model were based on five participants with an average age of 26 ±3 years, height of 177 ±3 cm, and weight of 70.1 ±7.8 kg. All anthropometric data were recorded using stereometrics outlined by McConville (1980) [106]. Body segment lengths were taken from Delp et al. (1990) [65]. Inertial parameters for the model can be found in Appendix C.

The model was scaled before any computations occurred. A scaling factor was created to match the distance between each of the virtual markers in the model to that of the experimental markers placed during the gait test. The mass of each limb segment was also adjusted based on a predetermined scaling factor to match the total mass of the participant. These adjustments affect inertial tensors of each limb segment to accurately represent each participant.

Once the model was scaled, residual reduction algorithm (RRA) was performed to minimize error that occurs during data collection and editing. Noise, model assumptions, and error from data collection can lead to dynamic inconsistency; the GRFs do not match up with the accelerations in the kinematic data. This will cause Newton's Second Law, $F = m * a$, to be false within the model. To rectify this issue, residual forces are created to balance the equation. RRA starts by using inverse kinematics to create force actuators to allow the model to move from the start to end position. These actuators generate the smallest necessary forces and torques for the model to reach its next position. The average value for each actuator was calculated. The model may have a slight lean to it due to how the specific subject's mass is distributed throughout the torso. To correct this, the averages of the internal joint torque through the sagittal plane ($\mathbf{M_x}$) and frontal

plane (**$M_z$**) were used to adjust the torso's center of mass (CoM). A new model with the updated center of mass was then created. The model's motion was simulated again, with the updated CoM and restrictions placed on the residual actuators. The restrictions were established to ensure the residual forces were large enough to simulate the movement accurately and small enough so they would not diminish any contribution from muscle forces or internal JRF.

Static optimization was the last process to occur within the model. Inverse dynamics is used to calculate joint torque moments from the given kinematic and kinetic data. The moments were then used to calculate individual muscle forces given the following constraints:

$$\sum_{m=1}^{nm}\left[a_m f\left(F_m^0, l_m, v_m\right)\right] r_{m,j} = \tau_j$$

Where *nm* is the number of muscles in the model, $\tau_j$ is the moment calculated using inverse dynamics, and $r_{m,j}$ is the moment arm about the joint axis. $f\left(F_m^0, l_m, v_m\right)$ is a function of a muscle's mechanical response based on Hill's elastic muscle model that contains a contractile element, series element, and parallel element. The variables it takes into consideration are the shortening velocity $(v_m)$, muscle length $(l_m)$, and maximum isometric force of the muscle $F^0_m$. The output is a value of force the muscle has generated during movement [70]. All of this occurs while minimizing metabolic effort which can be represented by:

$$J = \sum_{m=1}^{nm} (a_m)^p$$

where $J$ is the objective function, $a_m$ is muscle activation specific to a muscle defined by $m$, and $p$ is a user-defined constant that is set to 2. Due to the number of muscles that are included in this model, it is possible for the same torques to be created by a theoretical infinite amount of variations of muscle activation. The above equation absolves this redundancy by minimizing the required level of activation for each muscle while still yielding the correct torques [69].

**Figure 4:** OpenSim model with all observed muscles.

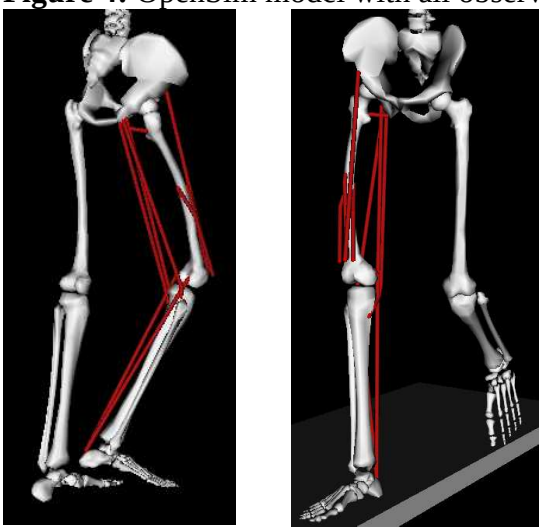

## Statistics

Baseline demographic characteristics for phase I were presented by OA status using means and standard deviations for continuous variables and counts and percentages for discrete variables. A mixed linear model approach controlling for age, and gender was used to compare characteristics across OA groups, and to estimate biomechanical gait characteristics. Within-subject variability across both legs was controlled by treating the study subject ID as a random effect. Gait data were plotted by OA status using smoothed averaged values over the percent gait cycle.

Phase II baseline demographic characteristics were also estimated using means and standard deviations for continuous variables and counts and percentages for discrete variables. Muscle forces were estimated using each of OpenSim and the DeVita models and values were compared using mixed model approach controlling for within person variability so that the main effect comparison for method estimates the mean difference between methods. Force data were plotted by the type of musculoskeletal model using smoothed averaged values over the percent gait cycle. All statistics were run in SAS v9.4 developed by SAS Institute, Cary, NC. Graphs were created using Microsoft Excel 2013 v15.

## Results

The first aim of this study was to compare the gait mechanics of older adults with radiographic and symptomatic knee OA (OA) to a matched population with symptomatic but no radiographic evidence of OA (non-OA). Standard deviations and mean values of the selected descriptive characteristics for both cohorts are noted in Table 1.

The non-OA group was younger with a mean age of 58 years compared to 65 years for the OA group. The non-OA group also had a lower mean BMI of 28.8kg/$m^2$ than the OA group who had a mean BMI of 30.1 kg/$m^2$. The non-OA group reported less pain and better function with a mean WOMAC pain score of 5.8 and a mean WOMAC function score of 19.2. This differs from the OA groups reported 7.3 mean pain and 29.6 mean function score. Walking speeds were similar between the groups, 1.26m/s for the non-OA group and 1.22m/s for the OA group. Gender distribution was 50% female for non-OA group and 53% female for the OA group. The OA group tended to have more comorbidities with 40% diagnosed other forms of arthritis, 53.3% with hypertension, and 6.7% with cardiovascular disease (CVD), compared to 33% with other forms of arthritis, 33% with hypertension, and 0% with CVD in the OA group.

Temporal, kinematic, and kinetic variables were compared between the groups. The temporal variables were stride length, stride rate, and walking speed. Kinematic variables included flexion/extension angle of the hip and knee, and plantar/dorsi flexion angle of the ankle. Kinetic variables included internal adduction/abduction moments of the hip and knee, internal extension/flexion moments of the hip, knee, and ankle, and total moment in the sagittal plane. Total power was also calculated.

**Table 1:** Descriptive statistics of participants without radiographic knee OA and with knee pain (Non-OA), and with both radiographic knee OA and knee pain (OA).

| | Non-OA (N=6) | | OA (N=15) | |
|---|---|---|---|---|
| | **Total** | **%** | **Total** | **%** |
| **Gender (# of Females)** | 3 | 50 | 8 | 53 |
| **# w/ Other Arthritis (N)** | 2 | 33 | 6 | 40 |
| **# w/ Hypertension (N)** | 2 | 33 | 8 | 53.3 |
| **# w/ CVD (N)** | 0 | 0 | 1 | 6.7 |
| | **Mean** | **SD** | **Mean** | **SD** |
| **Age (years)** | 58 | 7.2 | 65 | 5.7 |
| **BMI** | 28.8 | 4.5 | 30.1 | 3.6 |
| **WOMAC Pain** | 5.8 | 2.2 | 7.3 | 2.4 |
| **WOMAC Function** | 19.2 | 9.8 | 29.6 | 6.2 |
| **Walking Speed (m/s)** | 1.26 | 0.08 | 1.22 | 0.05 |

Hip and ankle ROM were similar between both groups with the non-OA group having a mean hip ROM of 40.2° and ankle ROM of 20.4° compared to the OA group who had 40.4°, and 20.6° mean angles, respectively. Knee ROM was also similar between groups. The non-OA group had a stride length of 1.35m while the OA group had a comparable stride length of 1.38m. The stride rate of the non-OA group was 55.4strides/min and 52.8strides/min for the OA group.

Hip, knee, and ankle angles are displayed in Figure 5a-c. Both groups follow a similar trend while the non-OA group had a slightly higher magnitude in the hip and knee angle.

**Table 2:** Temporal and kinematic comparison of participants who have knee pain with radiographic OA (OA) to those who have knee pain without radiographic OA (Non-OA).

| Variable | Non-OA | | OA | | |
|---|---|---|---|---|---|
| | **Mean** | **SE** | **Mean** | **SE** | **P-value** |
| **Stride Length (m)** | 1.35 | 0.05 | 1.38 | 0.03 | 0.72 |
| **Stride Rate (stride/min)** | 55.4 | 2.10 | 52.8 | 1.26 | 0.34 |
| **Hip ROM (deg)** | 40.2 | 1.6 | 40.4 | 0.96 | 0.93 |
| **Knee ROM (deg)** | 63.3 | 2.5 | 60.2 | 1.51 | 0.33 |
| **Ankle ROM (deg)** | 20.4 | 1.6 | 20.6 | 0.93 | 0.92 |

The non-OA group has a slightly higher (p=0.11) peak hip adduction moment at 0.99N*m/kg compared to the OA group at 0.83N*m/kg. Peak knee adduction moment was similar between the groups with a peak value of 0.46N*m/kg for the non-OA group and 0.42N*m/kg for the OA group. Total moment in the sagittal plane was slightly higher in the non-OA group at 0.83N*m/kg compared to the OA group at 0.51N*m/kg. Total power in the sagittal plane was 2.88W/kg for the non-OA and 2.29W/kg for the OA group (p = 0.26).

**Figure 5a-c:** Mean Hip, and Knee flexion/extension, and Ankle dorsi/plantar flexion ROM, of the affected leg for participants with knee pain and radiographic knee OA (OA) compared to participants with knee pain but no radiographic OA (Non-OA).

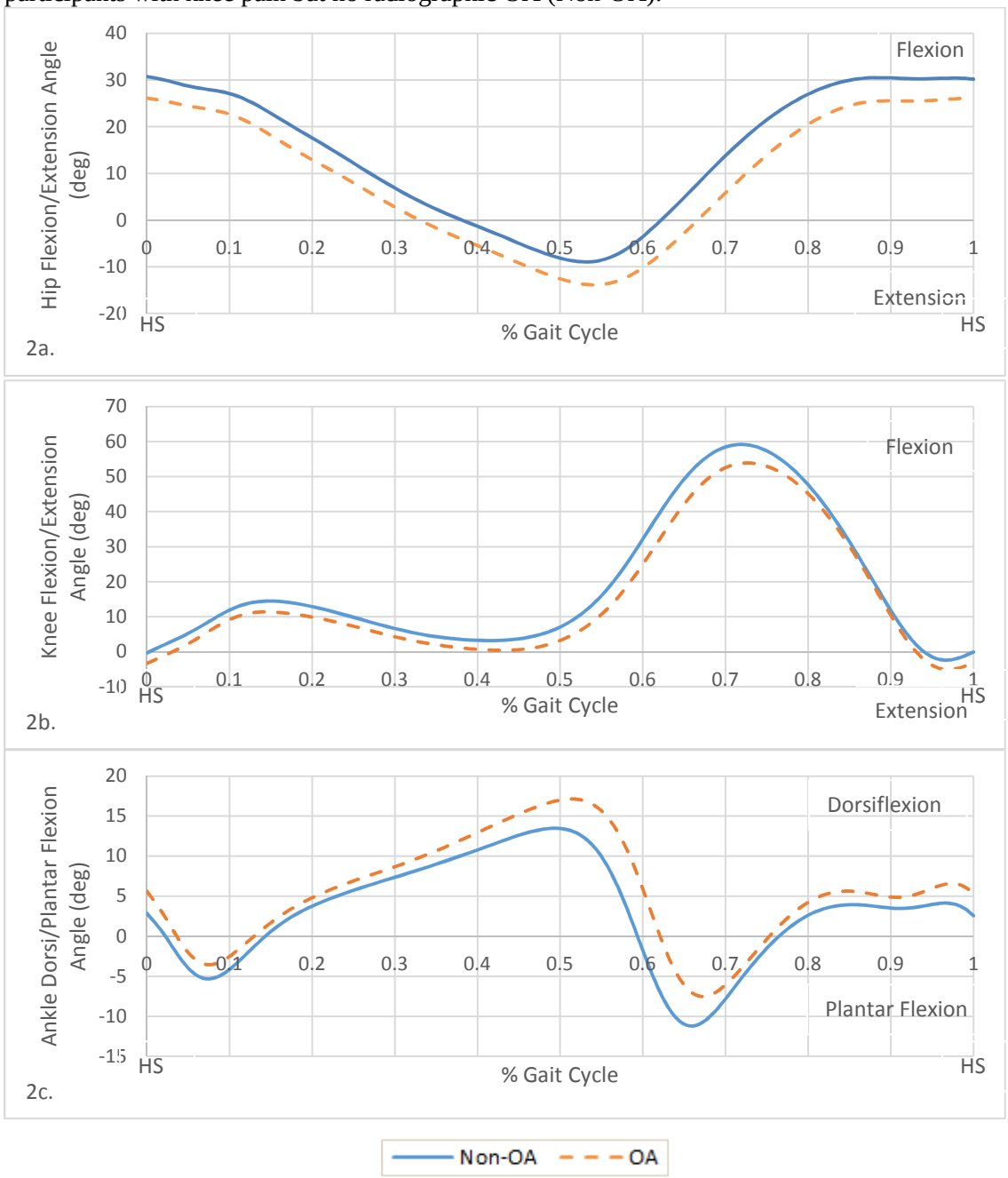

**Table 3:** Comparison of peak total power, abduction, and total moment in the sagittal plane of Participants who have Knee Pain with Radiographic OA (OA) to those who have Knee Pain without Radiographic OA (Non-OA) controlling for age, gender, and leg dominance.

| Variable | Non-OA | | OA | | |
|---|---|---|---|---|---|
| | **Mean** | **SE** | **Mean** | **SE** | **P-value** |
| **Hip Abduction Moment (N*m/kg)** | 0.99 | 0.08 | 0.83 | 0.05 | 0.11 |
| **Knee Abduction Moment (N*m/kg)** | 0.46 | 0.08 | 0.42 | 0.05 | 0.71 |
| **Total Moment-sagittal plane (N*m/kg)** | 0.83 | 0.10 | 0.51 | 0.06 | 0.02 |
| **Total Power-sagittal plane (W/kg)** | 2.88 | 0.41 | 2.29 | 0.25 | 0.26 |

**Figure 6a-f:** Mean hip, & knee abduction/adduction moments, hip, knee, and ankle extension/flexion moments, and total moment in the sagittal plane of the affected leg for participants with knee pain and radiographic knee OA (OA) compared to participants with knee pain but no radiographic OA (Non-OA).

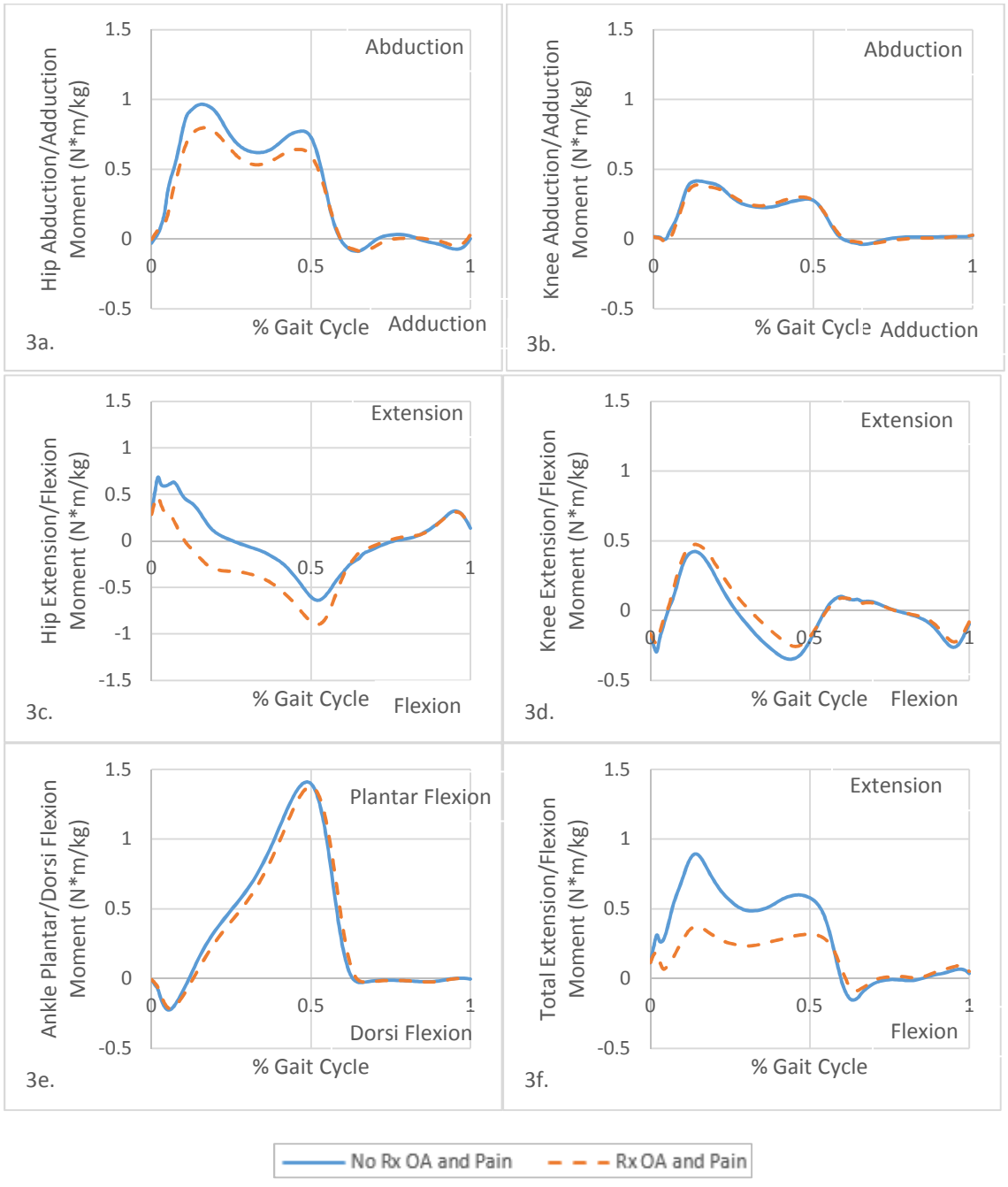

**Figure 7a-d:** Mean hip, knee, ankle, and total power in the sagittal plane of the affected leg for participants with knee pain and radiographic knee OA (OA) compared to participants with knee pain but no radiographic OA (Non-OA).

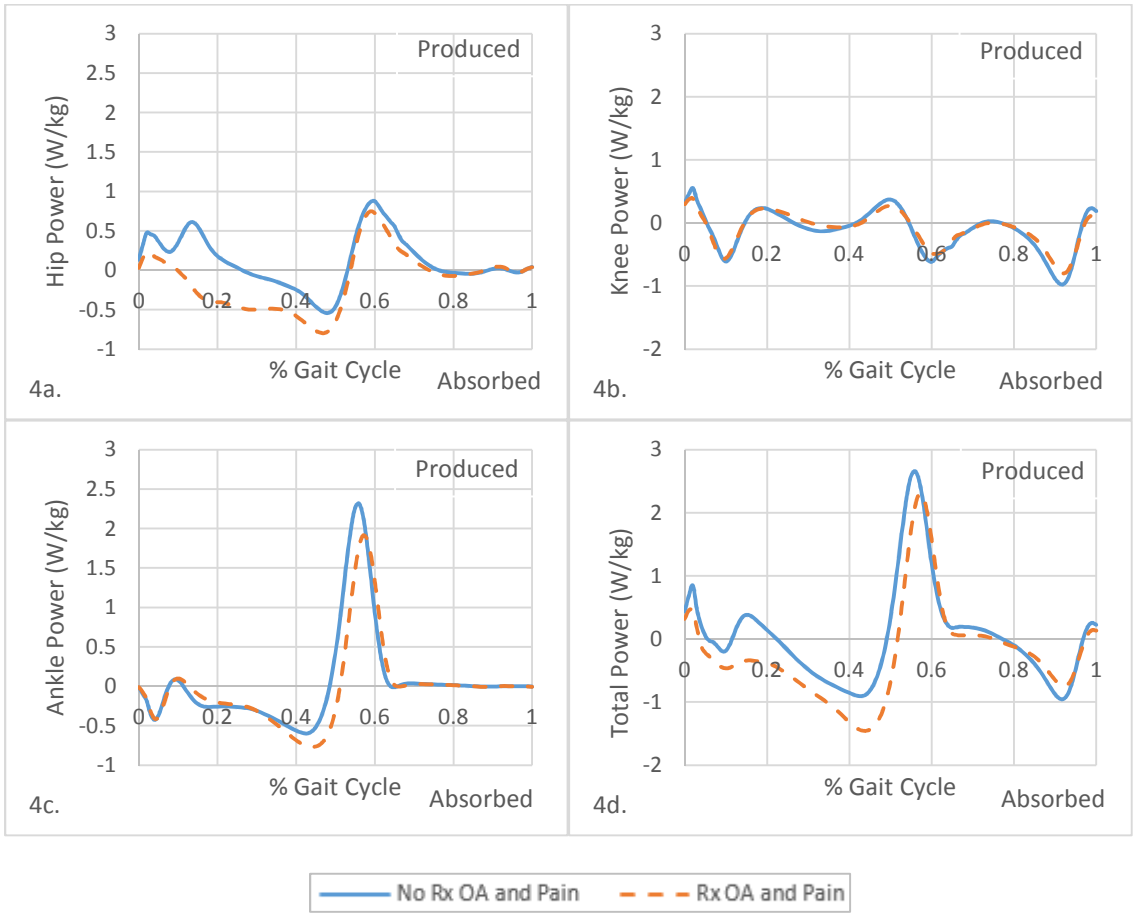


The two groups follow similar trends for all moments except the total moment in the sagittal plane which was larger in the non-OA group. The hip adduction/abduction and hip extension/flexion moments had a slightly larger magnitude in the non-OA group. The non-OA group had a larger hip and total power in the sagittal plane throughout the first 50% of the gait cycle. Both groups followed the same trend in knee power. The non-OA group had a slight higher ankle power between 40%-50% of the gait cycle, but otherwise followed the same trend as the OA group.

The second aim of the study was to compare the shear, compressive, quadriceps, hamstring, and gastrocnemius forces between the DeVita and OpenSim musculoskeletal models. The mean values and standard deviations for the descriptive characteristics of the population are shown in Table 4.

**Table 4:** Descriptive statistics for START cohort used in Phase II (N=31).

| Description | **Total** | **%** |
|---|---|---|
| **Gender (# of Females)** | 14 | 47 |
| **# w/ Other Arthritis (N)** | 13 | 43 |
| **# w/ Hypertension (N)** | 14 | 47 |
| **# w/ CVD (N)** | 8 | 27 |
| | **Mean** | **SD** |
| **Age (Years)** | 68.5 | 7.9 |
| **BMI (kg/m²)** | 27 | 2 |
| **Body Mass (kg)** | 76.6 | 10.3 |
| **Gait Speed (m/s)** | 1.35 | 0.24 |
| **WOMAC Pain** | 6.6 | 2.3 |
| **WOMAC Function** | 25 | 8 |

The mean age of the cohort was 68.5 years with a BMI of 27 and an average weight of 76.6 kg. The average gait speed was 1.35m/s. The mean WOMAC scores were 6.6 for pain and 25 for function; 47% of the cohort was female; 43% had some other form of arthritis; 47% had hypertension; 27% had CVD.

Kinetic variables were compared between the two models and consisted of knee compressive force, knee anteroposterior force, hamstring muscle force, quadriceps muscle force, and gastrocnemius muscle force. OpenSim quadriceps force was calculated by summing the rectus femoris, vastus medialis, vastus lateralis, and vastus intermedius muscle forces. The hamstring force was determined in a similar fashion by adding the

semimembranosus, semitendinosus, and biceps femoris long head muscle forces. The gastrocnemius force was determined by adding the medial and lateral gastrocnemius muscle forces. All peak forces were significantly different between the two models and are summarized in Table 5 and Figure 8.

The AP shear peak force for the first 50% of stance was 350.5N for the DeVita model and 335.5N for the OpenSim model. The peak AP shear force over the second half of stance was 611.4N for the DeVita model and 308.7N for the OpenSim model. The peak compressive force over the first 50% of stance was 1998.3N for the DeVita model and 2038.4N for the OpenSim model. The OpenSim model had a much higher peak compressive force during the second half of stance at 2742.1N compared to the DeVita model at 1557.7N. Peak Quadriceps force was higher in the DeVita model at 1076.9N compared to OpenSim at 707.1N. The DeVita model had a lower peak hamstring force at 464.5N compared to the OpenSim model at 679.3N. The gastrocnemius force was much lower in the DeVita model at 692.3N compared to the OpenSim model at 1760.2N. All comparisons were significantly different ($p < .01$).

Most variables followed similar trends, but had different magnitudes. The OpenSim model has a much higher compressive force during the second half of stance compared to the DeVita model. For the shear force, the DeVita and OpenSim models were similar until after the first peak where the DeVita model did not decrease as severely as OpenSim and began increasing earlier. The DeVita model had a larger peak for the quadriceps, but became more similar to OpenSim after the first half of stance. For the hamstrings, the OpenSim model had the first peak earlier than the DeVita model with

a steeper slope. The gastrocnemius force increased at a much higher peak in OpenSim compared to the DeVita model.

**Table 5:** Comparison of peak knee bone-on-bone peak joint contact forces and knee muscle forces between DeVita and OpenSim musculoskeletal models. Mean weight = 749.9N.

| | DeVita | | OpenSim | | |
|---|---|---|---|---|---|
| Variable | **Mean** | **SE** | **Mean** | **SE** | **Mean Comparison P-value** |
| **AP Shear Force – 1st Peak (N)** | 350.5 | 24.7 | 335.5 | 36.9 | 0.55 |
| **AP Shear Force – 2nd Peak (N)** | 611.4 | 24.0 | 308.7 | 15.6 | <.01 |
| **Compressive Force – 1st Peak(N)** | 1998.3 | 87.1 | 2038.4 | 135.2 | 0.75 |
| **Compressive Force – 2nd Peak(N)** | 1557.7 | 58.6 | 2742.1 | 132.0 | <.01 |
| **Quadriceps Force (N)** | 1076.9 | 66.5 | 707.1 | 59.7 | <.01 |
| **Hamstring Force (N)** | 464.5 | 24.7 | 679.3 | 42.4 | <.01 |
| **Gastrocnemius Force (N)** | 692.3 | 24.6 | 1760.2 | 92.5 | <.01 |

**Figure 8:** Mean compressive, shear, quadriceps, hamstring, and gastrocnemius forces from DeVita and OpenSim models.

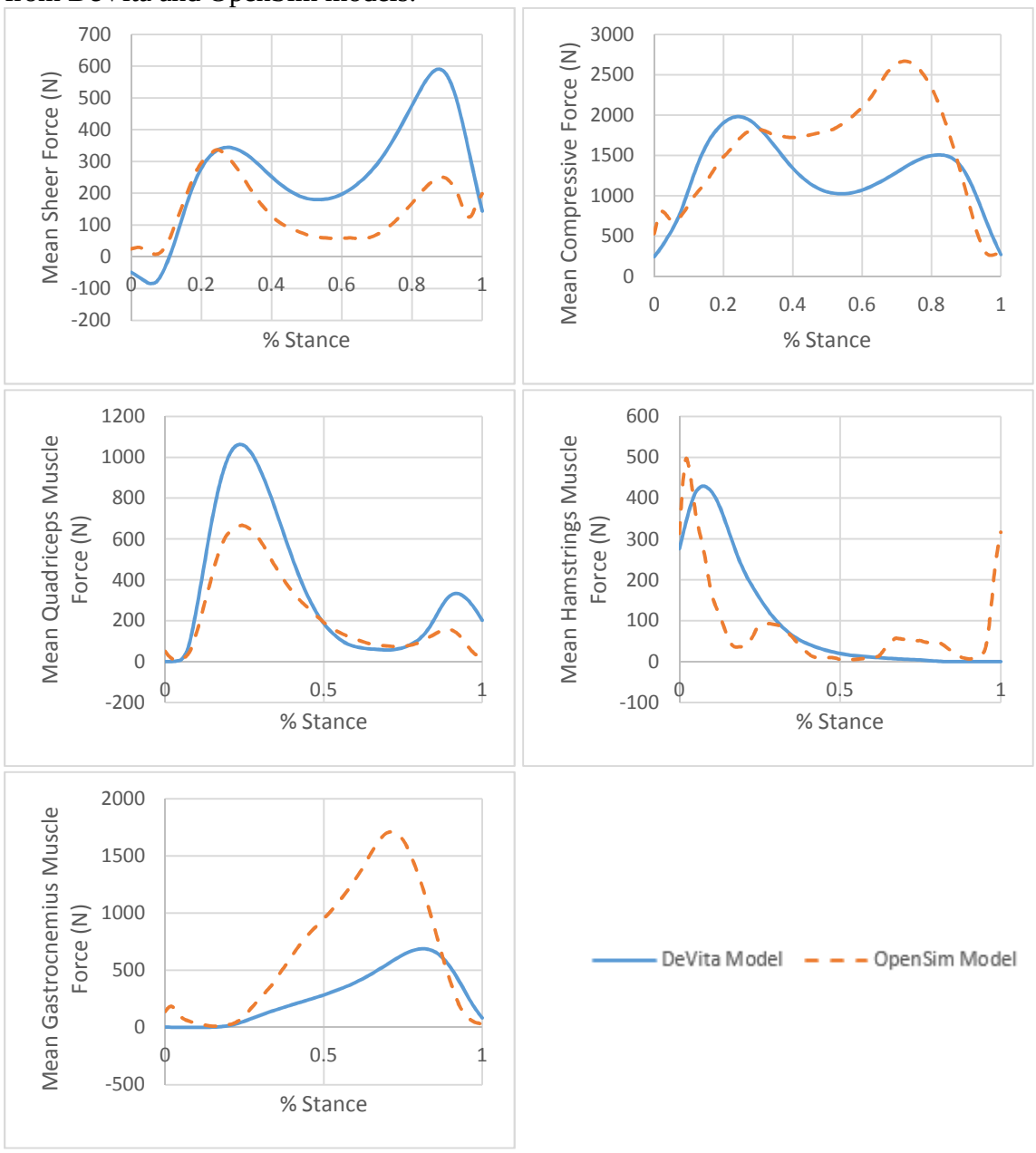

## Discussion

Our study consisted of two phases that each had their own set of participants, methodology, and overall goal. During the first phase, we compared gait between a population with radiographic knee OA and knee pain (OA) to a similar population with knee pain but no radiographic evidence of knee OA (non-OA). This pilot study was done to lay a foundation for future studies examining the same variables and whether gait is affected by radiographic evidence of OA.

We hypothesized the null, the gait characteristics of the OA and non-OA groups would not be significantly different. The results confirmed our hypothesis; total moment in the sagittal plane was the only variable of interest that was significantly different. We chose to hypothesize the null because we believed gait alterations in older adults with knee OA is an attempt to avoid or reduce pain in the affected joint. These altered gait characteristics occurred independent of the presence of OA.

To our knowledge, this is the first study to compare the effects of radiographic OA independent of pain on gait mechanics. Kinematic comparisons between the two groups were not significantly different. Previous studies have shown similar knee flexion angle and knee ROM values for a population with knee OA compared to our results. Baliunas et al. (2002) found a knee ROM of 58° (±7) for their radiographic knee OA population while Astephen et al. (2008) reported 66.0 (±7.40) for their moderate knee OA popualtion [97], [98]. These are similar to our findings with the OA group of 60.30° (±1.54) and the non-OA group of 63.12° (±2.57) knee ROM. Astephen et al. also reported ankle ROM (30.3° ±1.54) as well as the hip ROM (39.8° ±5.1) . The hip ROM coincides with our findings for both the OA (40.47° ±0.89) and non-OA (39.82° ±1.48)

groups, however, our ankle ROM tended to be lower for the OA group (20.47° ±0.91) and non-OA group (20.60° ±1.52) [98]. Overall, our values are consistent with previous literature.

Altered gait has been observed in participants with radiographic knee OA and knee pain, however, it is unclear if one contributes more than the other. Henriksen et al. found that healthy participants adopted a similar gait to those with knee OA after receiving injections of hypertonic saline into the infrapatellar fat pad [111]. This suggests that pain can contribute to altered gait and abnormal joint loading rather than just structural damage to the knee.

Phase II

The second phase of this study compared the muscle force output from the musculoskeletal model created by DeVita and Hortobagyi to the output generated from a model in SIMM OpenSim developed by Delp et al. [73], [65]. The OpenSim model is able to calculate individual muscle forces using residual reduction algorithm (RRA) and static optimization; however, it has not been used frequently with an older adult population that possesses an altered gait. The DeVita model has been used in multiple studies and bears validity with our population of interest [93],[99],[73]. The goal of this phase was to compare the output from these two models to offer a possible second option in calculating knee joint loads in future studies.

All variables observed in this section of the study were significantly different. Some of the variables had similar trends, particularly the quadriceps and shear forces seen in Figure 4, however, their magnitudes were different. The hamstring and gastrocnemius muscle forces had greater values for the OpenSim model. This difference

may be caused by the cost function used during static optimization. The current cost function optimizes muscle forces for normal gait and is being used for a special population that tries to reduce joint loading on the knee. This could potentially alter some of the muscles forces. The quadriceps was the only muscle force that had an overall lower magnitude in the OpenSim model. Xiao and Higginson also encountered relatively low vastus (VAS) activation when compared to recorded EMG signals (see in Figure 9) [104].

**Figure 9:** VAS excitation pattern compared to recorded EMG signals reported by Xiao and Higginson.

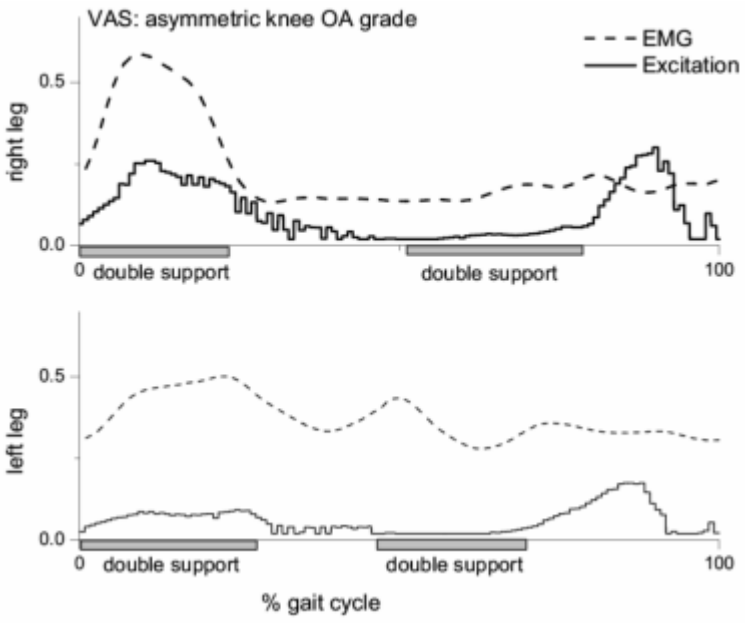


The gastrocnemius muscle force was much greater in the OpenSim model compared to the DeVita model. These disparities can be attributed to physiological differences in the population used to create the OpenSim model compared to the population of interest [101]. Physiological data from Anderson and Pandy (1990) was used to define muscle architecture in this OpenSim model. The average age of their population was 26 ±3 years compared to the average age of our population, 68.5 ±7.89 years [100]. To more accurately represent an older population, parameters such as max

muscle isometric force, tendon stiffness, max contraction velocity, would have to be adjusted [101]. There was not enough time to make these adjustments as they were only found after the study came to an end.

A quick test using the same methods as this study was performed on a younger participant to determine if the physiological differences were enough to have a major impact on the gastrocnemius muscle forces. The participant was 25 years old, and weighed 70.2kg and was 177.5cm tall. The young participant had a peak gastrocnemius force of 1481N while the older population from our study had 1760.2N. While the magnitude of the younger participant is lower, it is still very different from the results obtained from the DeVita model (Figure 10).

Bogert et al. used the OpenSim model on a younger population and found a peak gastrocnemius force of 25N/kg. Their participants had an average age of 28.3 ±3.9 years, and an average mass of 75.9 ±11.2kg. Their peak gastrocnemius force was about 1900N while ours was about 1700N for an older population with an average weight of 76.6kg [108]. This difference is likely due the older age and disability of our population.

Peak hamstring muscle force was greater in the OpenSim model compared to the DeVita model. Our OpenSim hamstring values were similar to values in the Bogert study, 6.5 N/kg vs 7.0 N/kg in the Bogert study. Bogert et al. used anthropometric data based on a model developed at the VA Rehabilitation R&D Center in Palo Alto California [107]. The OpenSim anthropometric data had 40% stronger gastrocnemius muscle force compared to the anthropometrics used by Bogert et al. While hamstring values differ, they follow the same pattern for both muscles and are relatively close when compared to

values derived from the DeVita model. Though the peak values differ between the two models, the muscle force patterns were similar.

**Figure 10:** Gastrocnemius muscle force compared between an older and younger population.

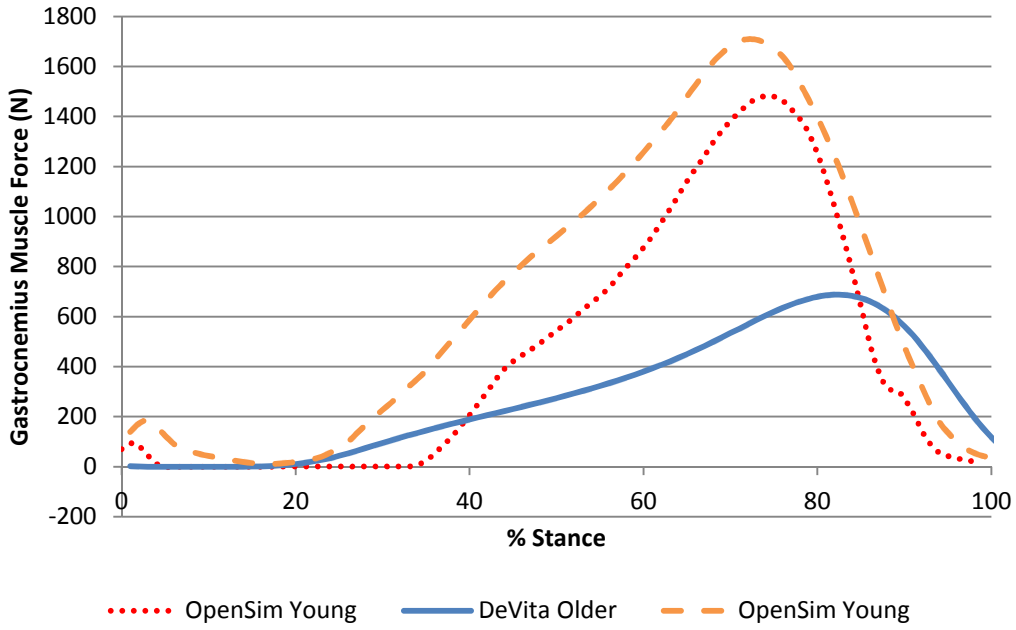


The results of the DeVita model are more comparable to results found in previous literature. Winby et al. found a peak gastrocnemius force of 840N, while Sasaki and Neptune reported a peak force of 860N for the same muscle [114], [115]. Pandy et al. found a higher gastrocnemius force of about 1,100N. These comparisons suggest that muscle force data from the DeVita model is more validated than that of the OpenSim model.

**Figure 11:** Medial and lateral muscle forces for the gastrocnemius and hamstring muscles found by Bogert et al.

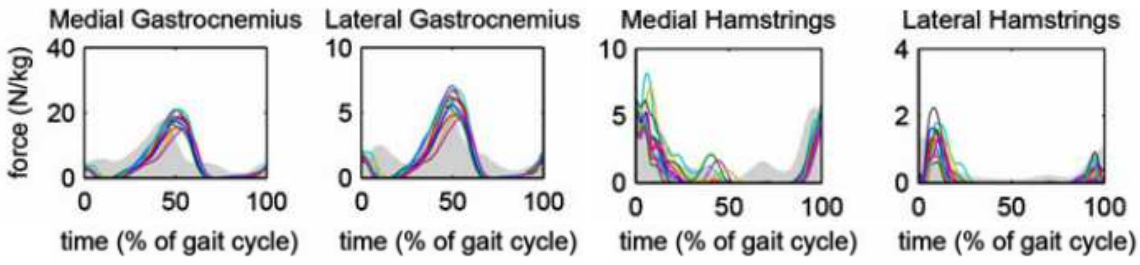

**Figure 12:** Quadriceps (——), hamstring (——), and gastrocnemius (– –) muscle forces determined by Winby et al. with an average body weight of 70kg.

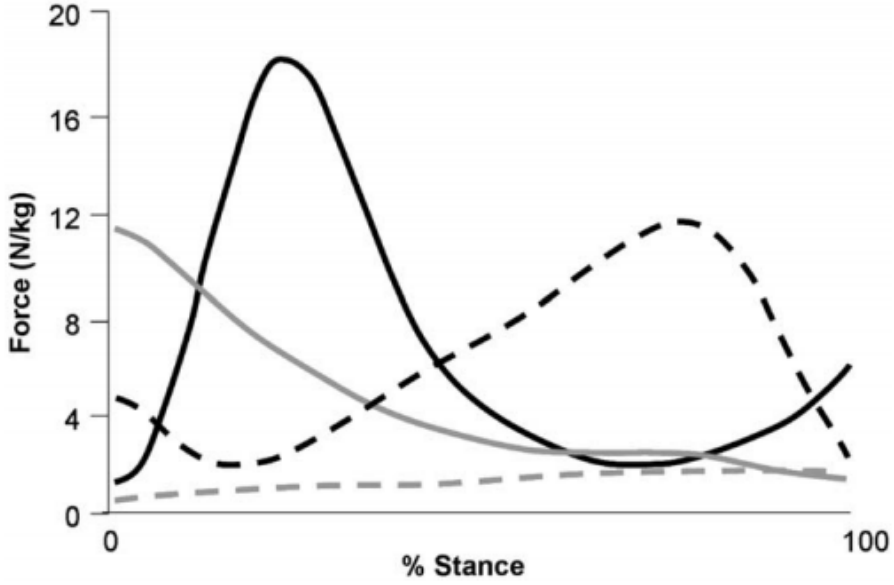


Limitations

A limitation to the first phase of the study was the number of participants in the non-OA group. The non-OA group only contained 6 participants. This makes any comparison between groups problematic as variability increases and power decreases.

Another limitation is the amount of adipose tissue on the participants, particularly around the hips. Excess adipose will further separate the center of the marker from the anatomical site it is intended to represent. The excess tissue will also move independently of the anatomical site resulting in unintended motion of the markers. Even with a mean BMI of 26.9 ±1.90, some participants had substantial adipose around the anterior-superior iliac spine and iliac crest. Implementing a new marker system that solves this issue may allow for more accurate placement of markers and reduce noise created by the adipose moving independently of the anatomical sites.

Further research regarding the OpenSim model is necessary before it is applied to an older adult population with knee OA. Thelen et al. suggests altered muscle parameters

that match an older population more than the current parameters. They estimated a 30% decrease in isometric strength for each muscle, a decrease in maximum contraction velocity by 20%, decrease in passive stiffness from 0.60 for the young adults to 0.50 for older adults, and an increase in deactivation time from 50ms to 60ms to more accurately reflect an older population [101].

Conclusions

There are few studies that have compared gait of an older adult with knee OA and knee pain to a similar population with knee pain and no knee OA. Our data show no significant differences in temporal, kinematic, and kinetic variables between the two populations. This pilot study was performed to lay a foundation for future studies that examine similar variables. A larger sample size is needed before definitive conclusions can be made.

The second phase compared the muscle forces of the DeVita and OpenSim models, and revealed similar patterns of muscle forces and knee joint forces, but significant difference in magnitudes. The advantage of using OpenSim is the inclusion of more knee muscles (N=9) compared to the DeVita model (N=3); however, the DeVita model has been used in many studies including OA patients and has been highly similar to direct knee joint measurements by Fregly et al. Currently, it is recommended to use the DeVita model over the OpenSim model due to its previously established validity. The muscle parameters of the OpenSim model should be adjusted outlined by Thelen et al. and undergo validation studies before being used in clinical research.

Appendix A**:** List of variables with their description and units.

| Variable | Unit | Description |
|---|---|---|
| **BMI** | - | Body Mass Index calculated by weight divided by height squared. |
| **Walk Speed** | m/s | Speed travelled across the runway. |
| **WOMAC Pain** | - | Level of pain determined by the Western Ontario and McMaster Universities Arthritis Index (WOMAC) questionnaire of a score range from 0-20 with a higher score indicating more pain. |
| **WOMAC Function** | - | Level of physical function determined by WOMAC questionnaire with a score range from 0-68 with a higher score indicating less function. |
| **Hip ROM** | Degrees | Difference between peak flexion in first 20% gait cycle and peak extension throughout all gait cycle. |
| **Knee ROM** | Degrees | Difference between peak flexion and peak extension over last 50% of gait cycle. |
| **Ankle ROM** | Degrees | Difference between peak plantar flexion and peak dorsi flexion over the first 50% gait cycle. |
| **Stride Length** | m | Distance traveled from heel strike to heel strike of the same foot. |
| **Stride Rate** | Stride/min | Number of strides completed within a minute. |
| **Adduction Moment** | N*m/kg | Moment through the frontal plane. |
| **VGRF** | N | Vertical force exerted on the knee joint. |
| **AP GRF** | N | Shear force generated in the knee joint in the anterior-posterior direction. |
| **Max Loading Rate** | N/kg*s | Loading rate is found as the derivative of the vertical component of ground reaction force normalized to body weight. Maximum loading rate is found between 20% and 80% of peak vertical ground reaction force. |

Appendix B: List of markers with anatomical location placement for both static and dynamic trials.

| **Description** | **Cortex Marker Name** | **Full Body – Walk** | **Full Body Static** | **Placement** |
|---|---|---|---|---|
| Left Lateral Knee<br>Right Lateral Knee | L. Knee Lateral<br>R. Knee Lateral | X | X | Along the flexion/extension axis of rotation on lateral femoral condyle |
| Left Medial Knee<br>Right Medial Knee | L. Knee Medial<br>R. Knee Medial | | X | Along the flexion/extension axis of rotation on medial femoral condyle |
| Left Lateral Ankle<br>Right Lateral Ankle | L. Ankle Lateral<br>R. Ankle Lateral | X | X | Along the flexion/extension axis of rotation on lateral malleolus |
| Left Medial Ankle<br>Right Medial Ankle | L. Ankle Medial<br>R. Ankle Medial | | X | Along the flexion/extension axis of rotation on medial malleolus |
| Upper L. Thigh Array<br>Front L. Thigh Array<br>Rear L. Thigh Array<br>Upper R. Thigh Array<br>Front R. Thigh Array<br>Rear R. Thigh Array | L. Thigh Upper<br>L. Thigh Front<br>L. Thigh Rear<br>R. Thigh Upper<br>R. Thigh Front<br>R. Thigh Rear | X | X | On the lower thigh below the mid-point, for best visibility by all cameras |
| Upper L. Shank Array<br>Front L. Shank Array<br>Rear L. Shank Array<br>Upper R. Shank Array<br>Front R. Shank Array<br>Rear R. Shank Array | L. Shank Upper<br>L. Shank Front<br>L. Shank Rear<br>R. Shank Upper<br>R. Shank Front<br>R. Shank Rear | X | X | On the lower shank below the mid-point, for best visibility by all cameras |
| Left Toe<br>Right Toe | L. Toe<br>R. Toe | X | X | Center of the foot between the 2nd and 3rd metatarsals |
| Left Heel<br>Right Heel | L. Heel<br>R. Heel | X | X | Posterior Calcaneus at same height from floor as toe marker |
| Left ASIS<br>Right ASIS | L. ASIS<br>R. ASIS | X | X | Anterior Superior Iliac Spine |
| Sacrum | V. Sacral | X | X | Superior Aspect of the L5-sacral interface |
| Left Scapula | L.Scapula | X | X | Inferior Aspect of the Scapula |
| Left Shoulder<br>Right Shoulder | L. Shoulder<br>R. Shoulder | X | X | Tip of the Acromion Process |
| Left Elbow<br>Right Elbow | L. Elbow<br>R. Elbow | X | X | Lateral Epicondyle of the Humerus |
| Left Wrist<br>Right Wrist | L. Wrist<br>R. Wrist | X | X | Centered between the styloid processes of the Radius and Ulna |
| Back of the Head<br>Front of the Head | Rear.Head<br>Front.Head | X | X | On the front and back of the head at the same height above the floor |
| Top of the Head | Top.Head | X | X | On the center of the head, in line with the front and back markers |
| **Additional Markers to be used for V3D** | | | | |
| Left PSIS<br>Right PSIS | L.Psis<br>R.Psis | | X | Posterior Superior Iliac Spine |
| Left Iliac Crest<br>Right Iliac Crest | L.Iliac.C<br>R.Iliac.C | | X | Most superior aspect of Illiac Crest |
| Left Greater Trochanter<br>Right Greater Trochanter | L.Troch<br>R.Troch | | X | On Greater Trochanter of the femur |

Appendix C: Inertial properties for OpenSim model.

| Body segment | Mass (kg) | Moments of inertia | | |
|---|---|---|---|---|
| | | xx | yy | zz |
| **Torso** | 34.2366 | 1.4745 | 0.7555 | 1.4314 |
| **Pelvis** | 11.777 | 0.1028 | 0.0871 | 0.0579 |
| **Right femur** | 9.3014 | 0.1339 | 0.0351 | 0.1412 |
| **Right tibia** | 3.7075 | 0.0504 | 0.0051 | 0.0511 |
| **Right patella** | 0.0862 | 0.00000287 | 0.00001311 | 0.00001311 |
| **Right talus** | 0.1000 | 0.0010 | 0.0010 | 0.0010 |
| **Right calcaneus** | 1.250 | 0.0014 | 0.0039 | 0.0041 |
| **Right toe** | 0.2166 | 0.0001 | 0.0002 | 0.0010 |
| **Left femur** | 9.3014 | 0.1339 | 0.0351 | 0.1412 |
| **Left tibia** | 3.7075 | 0.0504 | 0.0051 | 0.0511 |
| **Left patella** | 0.0862 | 0.00000287 | 0.00001311 | 0.00001311 |
| **Left talus** | 0.1000 | 0.0010 | 0.0010 | 0.0010 |
| **Left calcaneus** | 1.250 | 0.0014 | 0.0039 | 0.0041 |
| **Left toe** | 0.2166 | 0.0001 | 0.0002 | 0.0010 |

## References


1.
Frigg R, Hartmann S. Models in Science [Internet]. Summer 2009. Stanford Encyclopedia of Philosophy. Center for the Study of Language and Information, Stanford University: The Metaphysics Research Lab; 2006. Available from: http://plato.stanford.edu/archives/sum2009/entries/models-science/
2.
Pandy MG. Computer Modeling and Simulation of Human Movement. Annual Review of Biomedical Engineering. 2001;3(1):245–73.
3.
De Zee M, Lund ME, Schwartz C, Olesen CG, Rasmussen J. Validation of musculoskeletal models: the importance of trend validations. 2010 [cited 2013 Jul 15]; Available from: http://www.mech.kuleuven.be/iutam2010/IUTAM_proceedings/abstracts_invitedlecturers/IUTAM_de%20Zee.pdf
4.
Hamill J, Knutzen K. Hamill, Joseph, and Kathleen Knutzen. Biomechanical Basis of Human Movement. Philadelphia: Wolters Kluwer Health/Lippincott Williams and Wilkins, 2009. Print. 3rd ed. Lippincott Williams & Wilkins;
5.
Taylor KD, Mottier FM, Simmons DW, Cohen W, Pavlak Jr. R, Cornell DP, et al. An automated motion measurement system for clinical gait analysis. Journal of Biomechanics. 1982;15(7):505–16.
6.
Development C on VRR and, Board CS and T, Council NR. Virtual Reality: Scientific and Technological Challenges. National Academies Press; 1994.
7.
Burton K. Biomechanics of human movement: applications in rehabilitation, sports and ergonomics: N Berme and A Cappozzo, Eds Bertec Corp., Worthington, Ohio, 1990, 545 pp, $US56.50. [Bertec, 819 Loch Lomond Lane, Worthington, Ohio 43085, USA]. Clinical Biomechanics. 1992 Nov;7(4):251.
8.
Buchanan TS, Lloyd DG, Manal K, Besier TF. Estimation of Muscle Forces and Joint Moments Using a Forward-Inverse Dynamics Model: Medicine & Science in Sports & Exercise. 2005 Nov;37(11):1911–6.
9.
Erdemir A, McLean S, Herzog W, van den Bogert AJ. Model-based estimation of muscle forces exerted during movements. Clinical Biomechanics. 2007 Feb;22(2):131–54.
10.
Development and Validation of a Computational Musculoskeletal Model of the Elbow and Forearm - Springer. [cited 2013 Jul 15]; Available from: http://link.springer.com/article/10.1007/s10439-009-9637-x/fulltext.html
11.
Segal P, Jacob M. The Knee. Chicago. Year Book Medical Publishers; 1973.
12.

Wallace L. Orthopaedic and Sports Physical Therapy. St. Louis: Mosby; 1985.
13.
Radakovich M, Malone T. The Superior Tibiofibular Joint: The forgotten joint. Journal of Orthopaedic and Sports Physical Therapy. 1980;3:129–32.
14.
Platzer W. Color Atlas of Human Anatomy: Vol. 1, Locomotor System. Thieme; 2008.
15.
Fukubayashi T, Kurosawa H. The contact area and pressure distribution pattern of the knee: a study of normal and osteoarthrotic knee joints. Acta Orthopaedica. 1980;51(1-6):871–9.
16.
Radin EL, de Lamotte F, Maquet P. Role of the menisci in the distribution of stress in the knee. Clin Orthop Relat Res. 1984 May;(185):290–4.
17.
Yates J, Jackson D. Current status of meniscus surgery. Physician and Sports Medicine. 1984;12:51–6.
18.
Nisell R. Mechanics of the Knee: A study of joint and muscle load with clinical applications. Acta Othopaedica Scandivavica Supplemntum. 1985;56(216).
19.
Blackburn TA, Craig E. Knee Anatomy A Brief Review. Physical Therapy. 1980;60(12):1556–60.
20.
Lyon LK, Benz LN, Johnson KK, Ling AC, Bryan JM. Q-angle: a factor in peak torque occurrence in isokinetic knee extension*. J Orthop Sports Phys Ther. 1988;9(7):250–3.
21.
BRATTSTROEM H. SHAPE OF THE INTERCONDYLAR GROOVE NORMALLY AND IN RECURRENT DISLOCATION OF PATELLA. A CLINICAL AND X-RAY-ANATOMICAL INVESTIGATION. Acta Orthop Scand Suppl. 1964;68:SUPPL 68:1–148.
22.
Sharma L, Song J, Felson DT, Cahue S, Shamiyeh E, Dunlop DD. THe role of knee alignment in disease progression and functional decline in knee osteoarthritis. JAMA. 2001 Jul 11;286(2):188–95.
23.
Miyazaki T, Wada M, Kawahara H, Sato M, Baba H, Shimada S. Dynamic load at baseline can predict radiographic disease progression in medial compartment knee osteoarthritis. Ann Rheum Dis. 2002 Jul 1;61(7):617–22.
24.
Kettelkamp DB, Johnson RJ, Smidt GL, Chao EY, Walker M. An electrogoniometric study of knee motion in normal gait. J Bone Joint Surg Am. 1970 Jun;52(4):775–90.
25.
Lawrence RC, Felson DT, Helmick CG, Arnold LM, Choi H, Deyo RA, et al. Estimates of the prevalence of arthritis and other rheumatic conditions in the United States: Part II. Arthritis & Rheumatism. 2008;58(1):26–35.
26.

National Collaborating Centre for Chronic Conditions (Great Britain) RC of P of L, National Institute for Clinical Excellence (Great Britain). Osteoarthritis: national clinical guidelines for care and management in adults. London: Royal College of Physicians; 2008.
27.
Lawrence RC, Felson DT, Helmick CG, Arnold LM, Choi H, Deyo RA, et al. Estimates of the prevalence of arthritis and other rheumatic conditions in the United States: Part II. Arthritis & Rheumatism. 2008 Jan;58(1):26–35.
28.
Ray Fleming O of C and PL. Handout on Health: Osteoarthritis [Internet]. [cited 2013 Sep 16]. Available from: http://www.niams.nih.gov/Health_Info/Osteoarthritis/default.asp#2
29.
Spector TD, Hart DJ, Nandra D, Doyle DV, Mackillop N, Gallimore JR, et al. Low-level increases in serum C-reactive protein are present in early osteoarthritis of the knee and predict progressive disease. Arthritis Rheum. 1997 Apr;40(4):723–7.
30.
Sellam J, Berenbaum F. The role of synovitis in pathophysiology and clinical symptoms of osteoarthritis. Nature Reviews Rheumatology. 2010 Oct 5;6(11):625–35.
31.
Yuan G-H, Masuko-Hongo K, Sakata M, Tsuruha J-I, Onuma H, Nakamura H, et al. The role of C-C chemokines and their receptors in osteoarthritis. Arthritis & Rheumatism. 2001;44(5):1056–70.
32.
Harless E. The static moments of human limbs. Treatises of the Math -Phys Class of the Royal Acad of S. 1860;8:69–96, and 257–294.
33.
Buchanan TS. Technical Note Subject-Specific Estimates of Tendon Slack Length: A Numerical Method. Journal of Applied Biomechanics. 2004 May;20(2):195–203.
34.
Mazess RB, Barden HS, Bisek JP, Hanson J. Dual-energy x-ray absorptiometry for total-body and regional bone-mineral and soft-tissue composition. The American journal of clinical nutrition. 1990;51(6):1106–12.
35.
Creamer P, Lethbridge-Cejku M, Hochberg MC. Factors associated with functional impairment in symptomatic knee osteoarthritis. Rheumatology. 2000 May 1;39(5):490–6.
36.
Amin S, Goggins J, Niu J, Guermazi A, Grigoryan M, Hunter DJ, et al. Occupation-Related Squatting, Kneeling, and Heavy Lifting and the Knee Joint: A Magnetic Resonance Imaging-Based Study in Men. J Rheumatol. 2008 Aug;35(8):1645–9.
37.
Sandmark H, Hogstedt C, Vingård E. Primary osteoarthrosis of the knee in men and women as a result of lifelong physical load from work. Scandinavian Journal of Work, Environment & Health. 2000 Feb;26(1):20–5.
38.

Cooper C, McAlindon T, Coggon D, Egger P, Dieppe P. Occupational activity and osteoarthritis of the knee. Annals of the Rheumatic Diseases. 1994;53(2):90–3.
39.
Spector TD, MacGregor AJ. Risk factors for osteoarthritis: genetics. Osteoarthritis and Cartilage. 2004;12, Supplement:39–44.
40.
Valdes AM, Doherty M, Spector TD. The additive effect of individual genes in predicting risk of knee osteoarthritis. Ann Rheum Dis. 2008 Jan 1;67(1):124–7.
41.
Valdes AM, Loughlin J, Oene MV, Chapman K, Surdulescu GL, Doherty M, et al. Sex and ethnic differences in the association ofASPN,CALM1,COL2A1,COMP, andFRZB with genetic susceptibility to osteoarthritis of the knee. Arthritis & Rheumatism. 2007 Jan;56(1):137–46.
42.
Dillon CF, Rasch EK, Gu Q, Hirsch R. Prevalence of knee osteoarthritis in the United States: arthritis data from the Third National Health and Nutrition Examination Survey 1991-94. The Journal of rheumatology. 2006;33(11):2271–9.
43.
Davies-Tuck ML, Wluka AE, Wang Y, Teichtahl AJ, Jones G, Ding C, et al. The natural history of cartilage defects in people with knee osteoarthritis. Osteoarthritis and Cartilage. 2008 Mar;16(3):337–42.
44.
Felson DT, Goggins J, Niu J, Zhang Y, Hunter DJ. The effect of body weight on progression of knee osteoarthritis is dependent on alignment. Arthritis & Rheumatism. 2004 Dec;50(12):3904–9.
45.
Felson DT, Anderson JJ, Naimark A, Walker AM, Meenan RF. Obesity and Knee Osteoarthritis. Annals of Internal Medicine. 1988 7/1/88;109(1):18.
46.
Harrington IJ. Static and dynamic loading patterns in knee joints with deformities. J Bone Joint Surg Am. 1983 Feb;65(2):247–59.
47.
Johnson F, Leitl S, Waugh W. The distribution of load across the knee. A comparison of static and dynamic measurements. J Bone Joint Surg Br. 1980 Aug 1;62-B(3):346–9.
48.
Donelan JM, Kram R, Kuo AD. Mechanical and metabolic determinants of the preferred step width in human walking. Proc Biol Sci. 2001 Oct 7;268(1480):1985–92.
49.
Zhao D, Banks SA, Mitchell KH, D'Lima DD, Colwell CW, Fregly BJ. Correlation between the knee adduction torque and medial contact force for a variety of gait patterns. Journal of Orthopaedic Research. 2007;25(6):789–97.
50.
Kreighbaum E, Barthels K. Biomechanics: A Qualitative Approach for Studying Human Movement. 2nd ed. Burgess Publishing Company; 1981.
51.

Gordon T, Engel A. Osteoarthritis in us adults. Population Studies of the Rheumatic Disease. New York: Excerpta Medica Foundation; 1966. p. 391–7.
52.
Brandt KD, Dieppe P, Radin EL. Etiopathogenesis of Osteoarthritis. Rheumatic Disease Clinics of North America. 2008 Aug;34(3):531–59.
53.
Murphy L, Schwartz TA, Helmick CG, Renner JB, Tudor G, Koch G, et al. Lifetime risk of symptomatic knee osteoarthritis. Arthritis Care & Research. 2008;59(9):1207–13.
54.
Frontera W, Silver J, Rizzo T. Frontera: Essentials of Physical Medicine and Rehabilitation. 2nd ed. Philadelphia, Pa: Saunders Elsevier; 2008.
55.
Cappozzo A, Catani F, Della Croce U, Leardini A. Position and orientation in space of bones during movement: anatomical frame definition and determination. Clinical Biomechanics. 1995 Jun;10(4):171–8.
56.
Blackburn TA, Eiland G, Bandy WD. An introduction to the plica. J Orthop Sports Phys Ther. 1982;3(4):171–7.
57.
Kapandji IA. The Physiology of the Joints. Edinburgh: Churchill Livingstone; 1970.
58.
Takeya O, Cheryl R-K, Nancey B, Michele S, Shusaku K, Akira O. The Boundary of the Vastus Medialis Oblique and the Vastus Medialis Longus. J Phys Ther Sci. 2005;17(1):1–4.
59.
Saladin KS. Anatomy & Physiology: the unity of form and function. 5th ed. New York: McGraw-Hill; 2010.
60.
Ettinger WH Jr, Burns R, Messier SP, Applegate W, Rejeski WJ, Morgan T, et al. A randomized trial comparing aerobic exercise and resistance exercise with a health education program in older adults with knee osteoarthritis. The Fitness Arthritis and Seniors Trial (FAST). JAMA. 1997 Jan 1;277(1):25–31.
61.
Fisher NM, Pendergast DR. Effects of a muscle exercise program on exercise capacity in subjects with osteoarthritis. Arch Phys Med Rehabil. 1994 Jul;75(7):792–7.
62.
Analysis of effectiveness of therapeutic exercise for knee osteoarthritis and possible factors affecting outcome - Springer. [cited 2013 Oct 14]; Available from: http://link.springer.com/article/10.1007%2Fs00776-013-0443-9/fulltext.html
63.
Knoop J, Dekker J, van der Leeden M, van der Esch M, Klein P, Hunter D, et al. Is the severity of knee osteoarthritis on MRI associated with outcome of exercise therapy? Arthritis Care & Research. 2013 Aug;n/a–n/a.
64.
Andriacchi TP, Alexander EJ. Studies of human locomotion: past, present and future. Journal of Biomechanics. 2000 Oct;33(10):1217–24.

65.
Delp SL, Loan JP, Hoy MG, Zajac FE, Topp EL, Rosen JM. An interactive graphics-based model of the lower extremity to study orthopaedic surgical procedures. IEEE Transactions on Biomedical Engineering. 1990;37(8):757–67.
66.
St. Laurent AM. Understanding Open Source and Free Software Licensing. [Internet]. Sebastopol: O'Reilly Media, Inc.; 2008. Available from: http://public.eblib.com/EBLPublic/PublicView.do?ptiID=443485
67.
Hanavan Jr EP. A mathematical model of the human body [Internet]. DTIC Document; 1964. Available from: http://oai.dtic.mil/oai/oai?verb=getRecord&metadataPrefix=html&identifier=AD0608463
68.
Dempster WT, Gabel WC, Felts WJL. The anthropometry of the manual work space for the seated subject. American Journal of Physical Anthropology. 1959 Dec;17(4):289–317.
69.
Heintz S, Gutierrez-Farewik EM. Static optimization of muscle forces during gait in comparison to EMG-to-force processing approach. Gait & Posture. 2007 Jul;26(2):279–88.
70.
The biophysical foundations of human movement. 2nd ed. Champaign, IL: Human Kinetics; 2005.
71.
Rugg SG, Gregor RJ, Mandelbaum BR, Chiu L. In vivo moment arm calculations at the ankle using magnetic resonance imaging (MRI). Journal of Biomechanics. 23(5):495–7, 499–501.
72.
White SC, Yack HJ, Winter DA. A three-dimensional musculoskeletal model for gait analysis. Anatomical variability estimates. Journal of Biomechanics. 22(8-9):885–93.
73.
De Vita P, Hortobagyi T. Functional knee brace alters predicted knee muscle and joint forces in people with ACL reconstruction during walking. Journal of Applied Biomechanics. 2001;17(4):297–311.
74.
Yamaguchi GT, Zajac FE. A planar model of the knee joint to characterize the knee extensor mechanism. Journal of Biomechanics. 1989;22(1):1–10.
75.
Eggermont LHP, Bean JF, Guralnik JM, Leveille SG. Comparing Pain Severity Versus Pain Location in the MOBILIZE Boston Study: Chronic Pain and Lower Extremity Function. J Gerontol A Biol Sci Med Sci. 2009 Jul;64A(7):763–70.
76.
Amin S, Luepongsak N, McGibbon CA, LaValley MP, Krebs DE, Felson DT. Knee adduction moment and development of chronic knee pain in elders. Arthritis Care & Research. 2004;51(3):371–6.
77.

Ogata K, Whiteside LA, Lesker PA, Simmons DJ. The effect of varus stress on the moving rabbit knee joint. Clin Orthop Relat Res. 1977 Dec;(129):313–8.
78.
Studenski S, Perera S, Patel K, et al. Gait speed and survival in older adults. JAMA. 2011 Jan 5;305(1):50–8.
79.
Ounpuu S. The Biomechanics of Walking and Running. Clinics in Sports Medicine. 1994 Oct;13(4):843–63.
80.
Benedetti M, Catani F, Leardini A, Pignotti E, Giannini S. Data management in gait analysis for clinical applications. Clinical Biomechanics. 1998 Apr;13(3):204–15.
81.
Kaufman KR, Hughes C, Morrey BF, Morrey M, An K-N. Gait characteristics of patients with knee osteoarthritis. Journal of Biomechanics. 2001 Jul;34(7):907–15.
82.
Robertson DGE. Research Methods in Biomechanics. Human Kinetics; 2004. 326 p.
83.
Lloyd DG, Besier TF. An EMG-driven musculoskeletal model to estimate muscle forces and knee joint moments in vivo. Journal of Biomechanics. 2003 Jun;36(6):765–76.
84.
Steel, R.G.D., Torrie JH. Principles and Procedures of Statistics with Special Reference to the Biological Sciences. McGraw-Hill; 1960. 187-287 p.
85.
Thelen D, Ajay S, Anderson F, Delp S. OpenSim Gait 2392 and 2354 Models [Internet]. 2012. Available from: http://simtk-confluence.stanford.edu:8080/display/OpenSim/Gait+2392+and+2354+Models
86.
Brantigan OC, Voshell AF. The Mechanics of the Ligaments and Menisci of the Knee Joint. J Bone Joint Surg Am. 1941 Jan 1;23(1):44–66.
87.
Burr D, Radin E. Meniscal Function and the Importance of Meniscal Regeneration in Preventing Late Medial Compartment Osteoarthrosis. Current Orthopaedic Practice. 1982 Dec;171:121–6.
88.
Stredney D. The Representation of Anatomical Structures Through Computer Animation for Scientific, Educational and Artistic Applications. Ohio State University; 1982.
89.
Wickiewicz T, Roy R. Muscle Architecture of the Human Lower Limb. Orthopaedic Practice. 1983 Oct;179.
90.
Friederich JA, Brand RA. Muscle fiber architecture in the human lower limb. J Biomech. 1990;23(1):91–5.
91.
Hoy MG, Zajac FE, Gordon ME. A musculoskeletal model of the human lower extremity: the effect of muscle, tendon, and moment ann on the moment-angle relationship of

musculotendon actuators at the hip, knee, and ankle. Journal of Biomechanics. 1990;23:157–69.
92.
Vos et al., The lancet, Vol 380, December 15, 2012
93.
Messier SP, Legault C, Mihalko S, Miller GD, Loeser RF, DeVita P, et al. The Intensive Diet and Exercise for Arthritis (IDEA) trial: design and rationale. BMC Musculoskeletal Disorders. 2009 Jul 28;10(1):93.
94.
Herzog W, Nigg BM, Read LJ, Olsson E. Asymmetries in ground reaction force patterns in normal human gait. *Med Sci Sports Exerc*. 1989;21(1):110-114.
95.
McCrory JL, White SC, Lifeso RM. Vertical ground reaction forces: objective measures of gait following hip arthroplasty. *Gait Posture*. 2001;14(2):104-109.
96.
Giakas G, Baltzopoulos V, Dangerfield PH, Dorgan JC, Dalmira S. Comparison of gait patterns between healthy and scoliotic patients using time and frequency domain analysis of ground reaction forces. *Spine*. 1996;21(19):2235-2242.
97.
Baliunas AJ, Hurwitz DE, Ryals AB, Karrar A, Case JP, Block JA, et al. Increased knee joint loads during walking are present in subjects with knee osteoarthritis. Osteoarthritis and Cartilage. 2002 Jul;10(7):573–9.
98.
Astephen JL, Deluzio KJ, Caldwell GE, Dunbar MJ. Biomechanical changes at the hip, knee, and ankle joints during gait are associated with knee osteoarthritis severity. Journal of Orthopaedic Research. 2008 Mar;26(3):332–41.
99.
Messier SP, Mihalko SL, Legault C, et al. Effects of intensive diet and exercise on knee joint loads, inflammation, and clinical outcomes among overweight and obese adults with knee osteoarthritis: The idea randomized clinical trial. JAMA. 2013 Sep 25;310(12):1263–73.
100.
Anderson FC, Pandy MG. Dynamic Optimization of Human Walking. J Biomech Eng. 2001 May 16;123(5):381–90.
101.
Thelen DG. Adjustment of Muscle Mechanics Model Parameters to Simulate Dynamic Contractions in Older Adults. Journal of Biomechanical Engineering. 2003;125(1):70.
102.
Hunt MA, Birmingham TB, Giffin JR, Jenkyn TR. Associations among knee adduction moment, frontal plane ground reaction force, and lever arm during walking in patients with knee osteoarthritis. Journal of Biomechanics. 2006;39(12):2213–20.
103.
Lerner ZF, Board WJ, Browning RC. Effects of an Obesity-Specific Marker Set on Estimated Muscle and Joint Forces in Walking: Medicine & Science in Sports & Exercise. 2014 Jun;46(6):1261–7.
104.

Xiao M, Higginson J. Simulation study of walking patterns with knee osteoarthritis using opensim. American Society of Biomechanics Annual Meeting [Internet]. 2007 [cited 2014 Jul 22]. Available from: http://www.asbweb.org/conferences/2007/220.pdf
105.
Nisell R, Németh G, Ohlsén H. Joint forces in extension of the knee: analysis of a mechanical model. Acta Orthopaedica. 1986;57(1):41–6.
106.
McConville JT, Clauser CE, Churchill TD, Cuzzi J, Kaleps I. Anthropometric relationships of body and body segment moments of inertia [Internet]. DTIC Document; 1980. Available from: http://oai.dtic.mil/oai/oai?verb=getRecord&metadataPrefix=html&identifier=ADA097238
107.
Delp S. Musculotendon Parameters for Lower Limb Muscles [Internet]. Available from: http://isbweb.org/data/delp/Muscle_parameter_table.txt
108.
Van den Bogert AJ, Geijtenbeek T, Even-Zohar O, Steenbrink F, Hardin EC. A real-time system for biomechanical analysis of human movement and muscle function. Medical & Biological Engineering & Computing. 2013 Oct;51(10):1069–77.
109.
Srikanth VK, Fryer JL, Zhai G, Winzenberg TM, Hosmer D, Jones G. A meta-analysis of sex difference prevalence, incidence and severity of osteoarthritis. Osteoarthritis Cartilage. 2005;13:769-781.
110.
Henriksen M, Simonsen EB, Alkjær T, Lund H, Graven-Nielsen T, Danneskiold-Samsøe B, et al. Increased joint loads during walking – A consequence of pain relief in knee osteoarthritis. The Knee. 2006 Dec;13(6):445–50.
111.
Henriksen M, Graven-Nielsen T, Aaboe J, Andriacchi TP, Bliddal H. Gait changes in patients with knee osteoarthritis are replicated by experimental knee pain. Arthritis Care & Research. 2010 Apr;62(4):501–9.
112.
Fregly BJ, Besier TF, Lloyd DG, Delp SL, Banks SA, Pandy MG, et al. Grand challenge competition to predict in vivo knee loads. Journal of Orthopaedic Research. 2012 Apr;30(4):503–13.
113.
Messier SP, Mihalko SL, Beavers DP, Nicklas BJ, DeVita P, Carr JJ, et al. Strength Training for Arthritis Trial (START): design and rationale. BMC musculoskeletal disorders. 2013;14(1):208.
114.
Winby CR, Lloyd DG, Besier TF, Kirk TB. Muscle and external load contribution to knee joint contact loads during normal gait. Journal of Biomechanics. 2009 Oct;42(14):2294–300.
115.
Sasaki K, Neptune RR. Individual muscle contributions to the axial knee joint contact force during normal walking. Journal of Biomechanics. 2010 Oct;43(14):2780–4.

116.
Pandy MG, Andriacchi TP. Muscle and Joint Function in Human Locomotion. Annual Review of Biomedical Engineering. 2010 Jul;12(1):401–33.

# Josh Wallace

*jaywall606@gmail.com*
717-304-0036

Permanent Address:
11 Fox Run Road
Lebanon, PA 17042

---

## EDUCATION

**Wake Forest University**, Winston-Salem, NC, May 2014
Master of Science in Health & Exercise Science
Thesis: Gait Mechanics, Joint Contact Forces, and Muscle Forces in Older Adults with Radiographic Knee Osteoarthritis and Knee Pain compared to a similar Population with Knee Pain and no Radiographic Knee Osteoarthritis

**University of Delaware,** Newark, DE, May 2012
Bachelor of Science in Health & Exercise Science: Concentration in Human Physiology and Biomechanics
Awarded Most Outstanding Student in Health & Exercise Science Class of 2012.

## EXPERIENCE

**Lab Assistant**, J.B. Snow Biomechanics Lab, Wake Forest University, Fall 2012-Fall 2014

- Conducted research using a passive marker motion capture system and related software including: Cortex 3.0, Visual 3D, & OpenSim.

**Instructor**, Wake Forest University, Fall 2012-Spring 2014

- Prepared and taught lectures to undergraduates ranging from freshmen to seniors.

**Tutor**, Learning Assistance Center, Wake Forest University, Fall 2013

- Tutored students in an individual & group setting in biomechanics

**Interventionist**, Clinical Research Center, Wake Forest University, Fall 2012-Fall 2013

- Worked at HELPS, an exercise & healthy living program aimed at helping older adults with medical conditions (i.e. stroke, osteoarthritis, diabetes, etc.) exercise in a safe environment.

**Summer Scholars Recipient**, Human Performance Lab, University of Delaware, Summer 2011
Research & poster presentation on "Forearm Versus Upper Arm Blood Pressure Differences"

- Assisted with blood pressure data collection from participants during cardiac catheterization.
- Processed data using Labview and MATLAB.

**Research Assistant**, Human Performance Lab, University of Delaware, Summer 2010
Research on the "Effect of Footwear on Balance"

- Created & used programs to process and analyze collected data

## VOLUNTEER:

- Held an elected position of fundraising chair for a non-profit organization. Responsibilities included planning fundraising events for members to attend and encouraging attendance.
- Volunteered with many service related organizations ranging from the Food Bank to the SPCA.

## COMPUTER SKILLS:

- Previous experience with Visual 3D, and Labview.